

IEEE/NSS Lyon,
Oct. 15, 2000

Particle identification at high energies, Part 1

Peter Križan

*University of Ljubljana and J. Stefan Institute,
Ljubljana, Slovenia*

Part I

- Introduction: Why Particle ID?
- Basics: dE/dx , Cherenkov, Trans. Rad.
- Cherenkov radiation
- Types of Cherenkov counters
- RICH Designs: proximity and mirror focused
- Overview of RICH building blocks
- Short historical excursion
- Gas based detectors (TMAE, TEA, CsI)

Part II. Christian Joram

- Vacuum based Photo detectors: Requirements
- Photocathodes in the visible range
- Photomultipliers
- Hybrid Photodiodes
- Photocathode fabrication
- Applications
- Auxiliary systems (gas & liquid circulation, cleaning, monitoring of T and n)
- Alternatives: dE/dx , lifetime, TOF, exotics

Part III.

- Electron identification: introduction.
- Calorimeters: shower shape, granularity, pile-up effects, trigger.
- Energy/momentum matching; rejection against photon conversions.

Part IV. Daniel Froidevaux

- Transition radiation: principle and limitations.
- The ATLAS Transition Radiation Tracker.

Introduction: Why Particle ID?

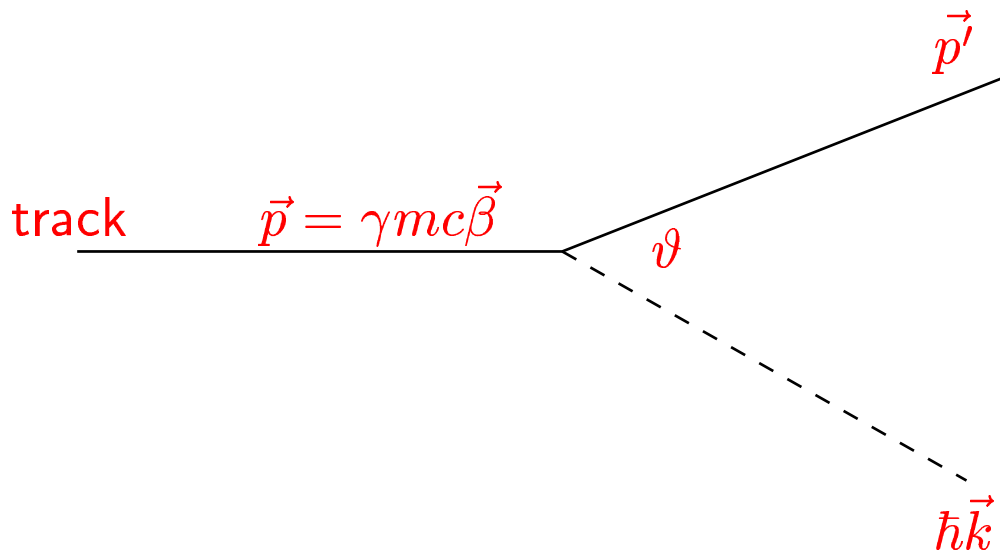
Particle identification is an important aspect of high energy physics experiments.

Some physical quantities are only accessible with sophisticated particle identification (B-physics, CP violation, rare exclusive decays).

Last decade: a boost in interest due to preparation of B-factories, hadron collider experiments, heavy ion experiments, upgrades of running spectrometers.

Basics: dE/dx , Čerenkov, Trans. Rad.

Charged particle of mass m and velocity $\vec{\beta}c$ interacts electromagnetically with detector medium via a photon of energy $\hbar\omega$ and momentum $\hbar\vec{k}$



Conservation of energy and momentum gives

$$\hbar\omega\left(1 - \frac{\hbar\omega}{2\gamma mc^2}\right) = \hbar\vec{k} \cdot \vec{\beta}c - \frac{\hbar^2 k^2}{2\gamma m}$$

typically $\hbar\omega \ll \gamma mc^2$ and $\hbar k \ll \gamma mc \rightarrow$

$$\omega = \vec{k} \cdot \vec{\beta}c = \beta ck \cos \vartheta. \quad (1)$$

The photon also has to satisfy the dispersion relation for a given medium with a dielectric constant ϵ

$$\omega^2 - \frac{k^2 c^2}{\epsilon} = 0 \quad (2)$$

From (1) and (2) we get

$$\sqrt{\epsilon} \beta \cos \vartheta = 1$$

which has a solution with a real value of ϑ if

$$\sqrt{\epsilon} \beta = n \beta > 1. \quad (3)$$

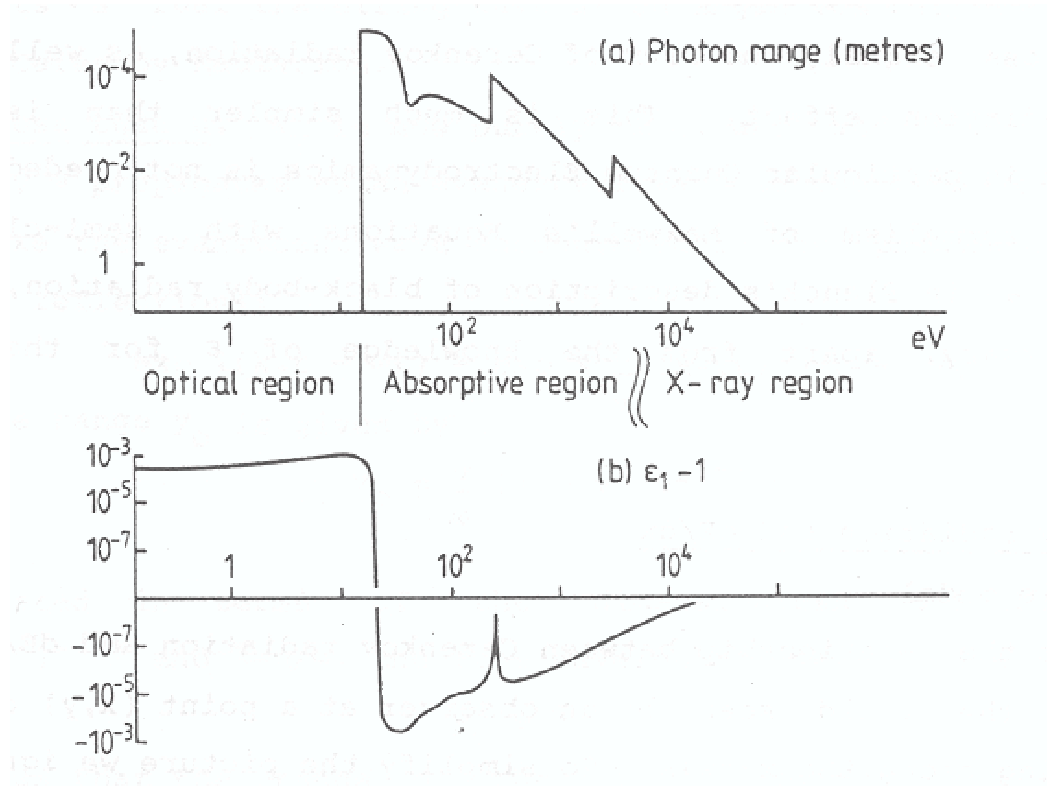
In this case **real** (Čerenkov) photons are emitted, and the emission angle is called Čerenkov angle ϑ_c .

N.B. In discontinuous media diffraction causes real photon emission even if (3) is not fulfilled (transition radiation).

Cross-section for emission (see Appendix for details)

$$\begin{aligned} \frac{d\sigma}{d(\hbar\omega)} &= \frac{\alpha}{\beta^2 \pi} \frac{\sigma_\gamma(\hbar\omega)}{\hbar\omega Z} \log \left[(1 - \beta^2 \epsilon_1)^2 + \beta^4 \epsilon_2^2 \right]^{-\frac{1}{2}} \\ &+ \frac{\alpha}{\beta^2 \pi} \frac{\sigma_\gamma(\hbar\omega)}{\hbar\omega Z} \log \left[\frac{2mc^2 \beta^2}{\hbar\omega} \right] \quad (\text{ionis., excit.} \rightarrow dE/dx) \\ &+ \frac{\alpha}{\beta^2 \pi} \frac{1}{n_e \hbar c} \left[\beta^2 - \frac{\epsilon_1}{|\epsilon|^2} \right] \Theta \quad (\text{Čerenkov, TRD}) \\ &+ \frac{\alpha}{\beta^2 \pi} \frac{1}{(\hbar\omega)^2} \int_0^{\hbar\omega} \frac{\sigma_\gamma(\hbar\omega')}{Z} d(\hbar\omega') \quad (\delta \text{ electrons}) \end{aligned}$$

Three frequency ranges:



1) **Optical region: ϵ real and > 1 .**

The medium is transparent. Čerenkov radiation is emitted by particles with velocity above the threshold.

2) **Absorptive region: ϵ complex.**

Imaginary part makes the range of photons short.

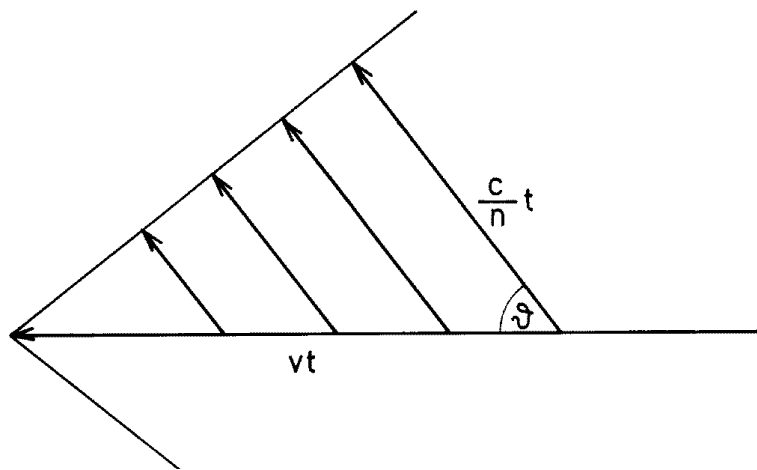
3) **X-ray region: ϵ nearly real and < 1 .**

Čerenkov threshold is greater than c but sub-threshold Čerenkov radiation can be emitted at discontinuities in the medium \rightarrow X-ray Transition Radiation.

Čerenkov radiation

A charged track with velocity $v = \beta c$ above the speed of light c/n in a medium with the index of refraction $n = \sqrt{\epsilon}$ emits **polarized** light at a characteristic (Čerenkov) angle,

$$\cos \vartheta = \frac{c/n}{v} = \frac{1}{\beta n}$$



Two cases:

1) $\beta < \beta_t = \frac{1}{n}$: below threshold no Čerenkov light is emitted.

2) $\beta > \beta_t$: the number of Čerenkov photons emitted over unit photon energy $E = \hbar\omega$ in a radiator of length L amounts to

$$\frac{dN}{dE} = n_e L \frac{d\sigma}{dE} = L \frac{\alpha}{\hbar c} \sin^2 \vartheta$$

where $\frac{\alpha}{\hbar c} = 370 \text{eV}^{-1} \text{cm}^{-1}$

Number of detected photons

Example: in 1 cm of water ($n = 1.33$) a track with $\beta = 1$ emits $N = 320$ photons in the spectral range of visible light ($\Delta E \approx 2$ eV).

If Čerenkov photons were detected with an average detection efficiency of $\epsilon = 0.1$ over this interval, $N = 32$ photons would be measured.

In general: number of detected photons amounts to

$$N = N_0 L \sin^2 \vartheta$$

where N_0 is the figure of merit,

$$N_0 = \frac{\alpha}{\hbar c} \int Q \cdot T \cdot R dE$$

and $Q \cdot T \cdot R$ is the product of photon detection efficiency, transmission of the radiator and windows and reflectivity of mirrors employed.

Typically: $N_0 = 50 - 100/\text{cm}$

Rewrite the basic relations:

- the threshold Lorentz factor $\gamma_t = (1 - 1/n^2)^{-1/2}$
- the asymptotic value of Čerenkov angle (for $\beta = 1$)
$$\sin^2 \theta_{max} = \frac{1}{\gamma_t}$$

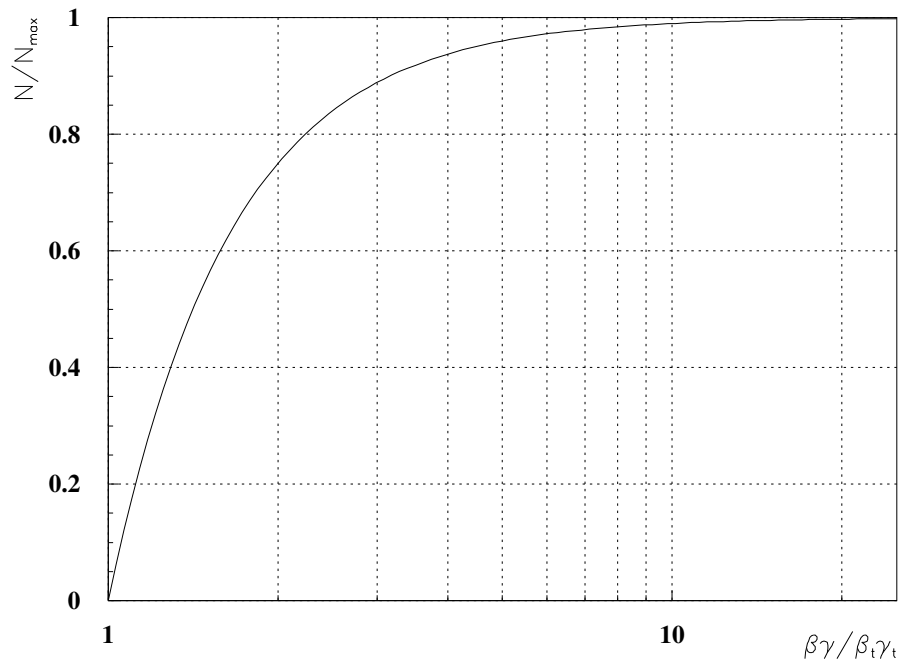
- the asymptotic number of Čerenkov photons:
$$N_{max} = \frac{N_0 L}{\gamma_t^2}$$

- number of photons, non-asymptotic case:
$$\frac{N}{N_{max}} = 1 - \frac{(\beta_t \gamma_t)^2}{(\beta \gamma)^2}$$

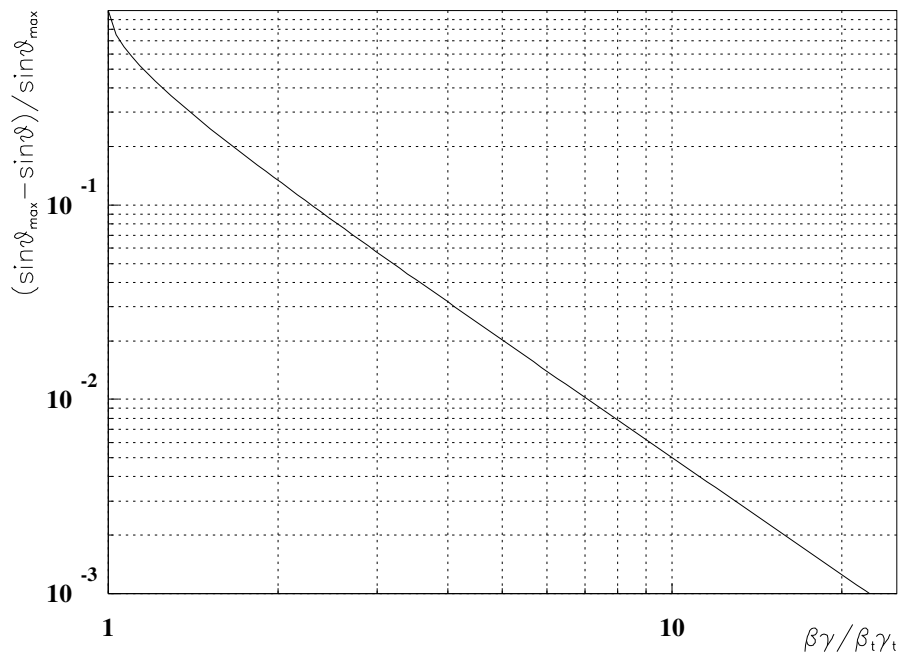
- Čerenkov angle, non-asymptotic case:
$$\frac{\sin \theta^2}{\sin \theta_{max}^2} = \sqrt{1 - \frac{(\beta_t \gamma_t)^2}{(\beta \gamma)^2}}$$

The basic relations are functions of the ratio $\frac{\beta \gamma}{\beta_t \gamma_t} = \frac{p}{p_t}$

Number of photons



Deviation from the maximum angle



Types of Čerenkov counters

Threshold counters

→ count photons to separate particles below and above threshold

Ring Imaging (RICH or CRID)

→ measure Čerenkov angle

→ count photons

Threshold Č. counters

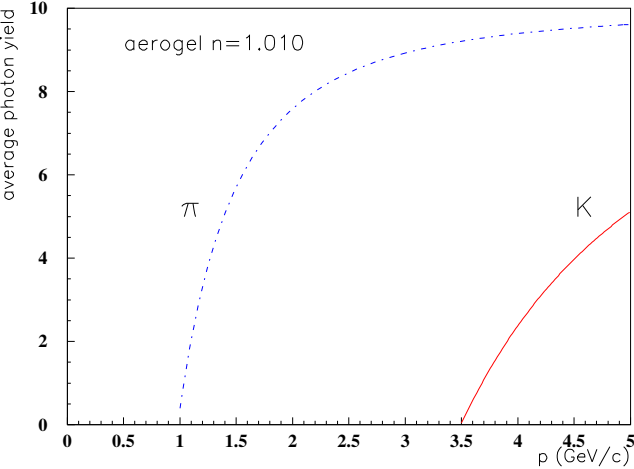
Beam veto counters

Detection of sub-threshold particles in a RICH

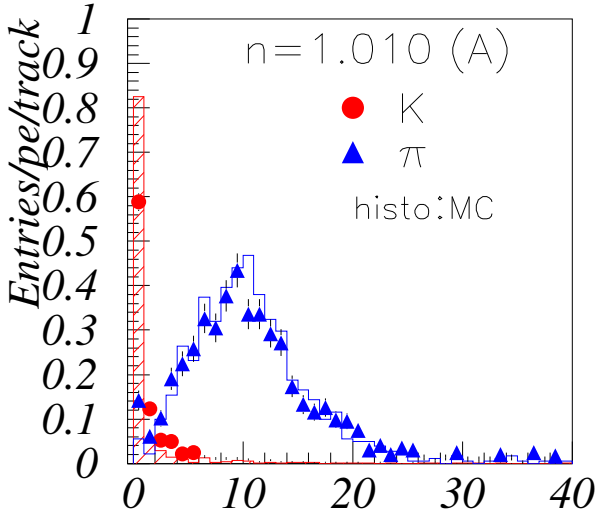
Aerogel Čerenkov counter

Belle: K (below) vs. π (above thr.) by properly choosing n for a given kinematic region

expected yield vs p



measured for $2 \text{ GeV} < p < 3.5 \text{ GeV}$

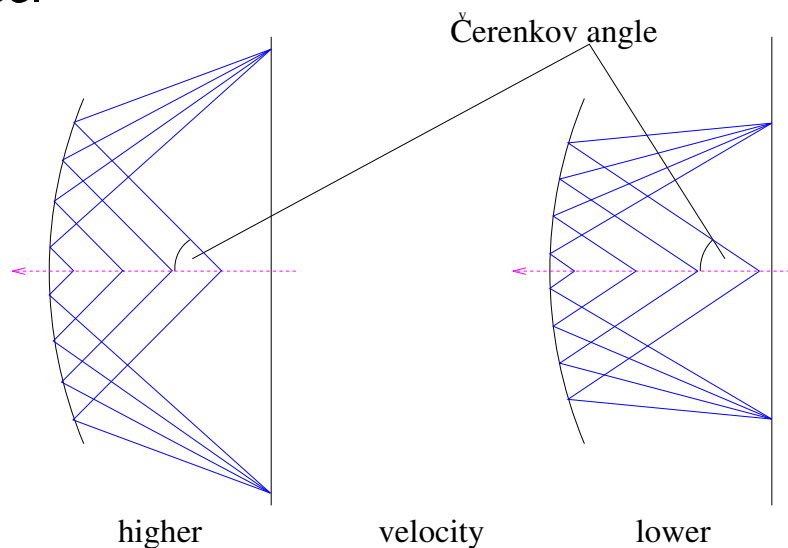


RICH counter

Aim: measure the direction of Čerenkov photons emitted by a charged track.

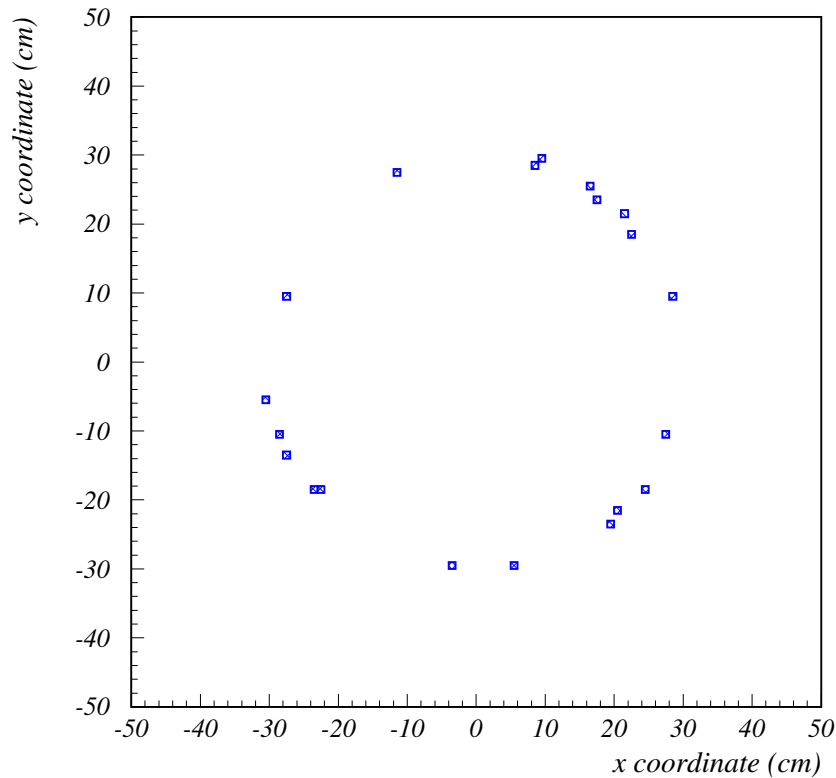
Idea: transform the **direction** into a **coordinate**.

Take a **spherical mirror**: parallel rays intersect on the focal surface.

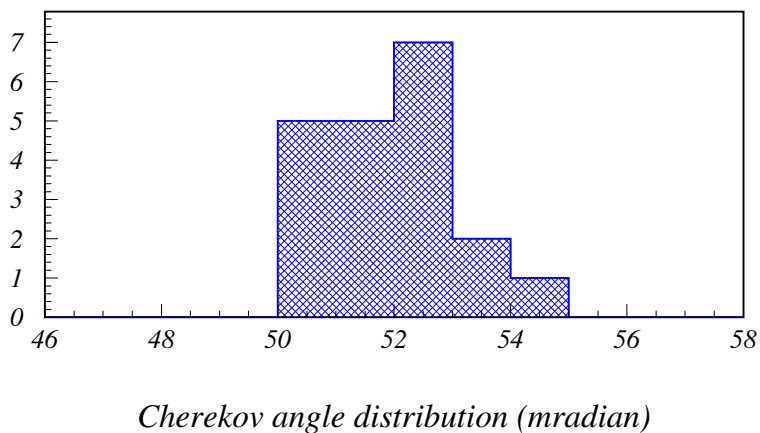


Since photons are emitted uniformly over the azimuthal angle around the track, a ring is formed on the focal plane.

With a **position sensitive photon detector** in the focal plane we get a **Ring Imaging Čerenkov counter (RICH)**

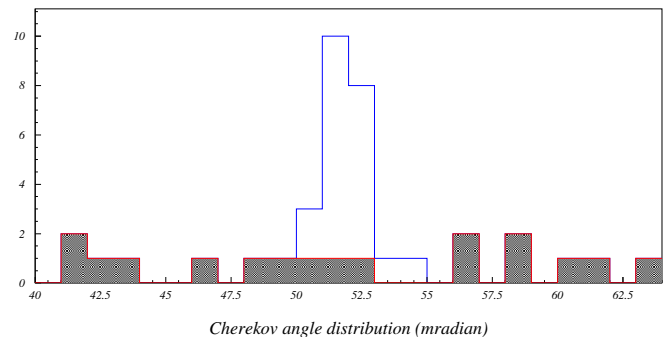
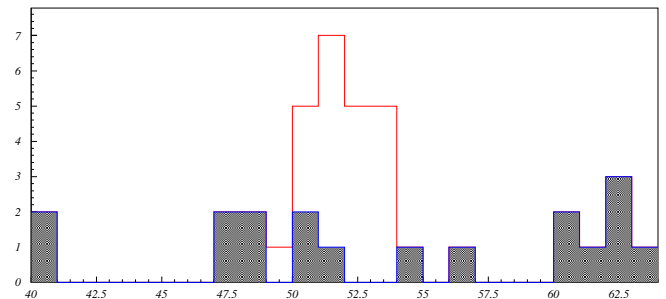
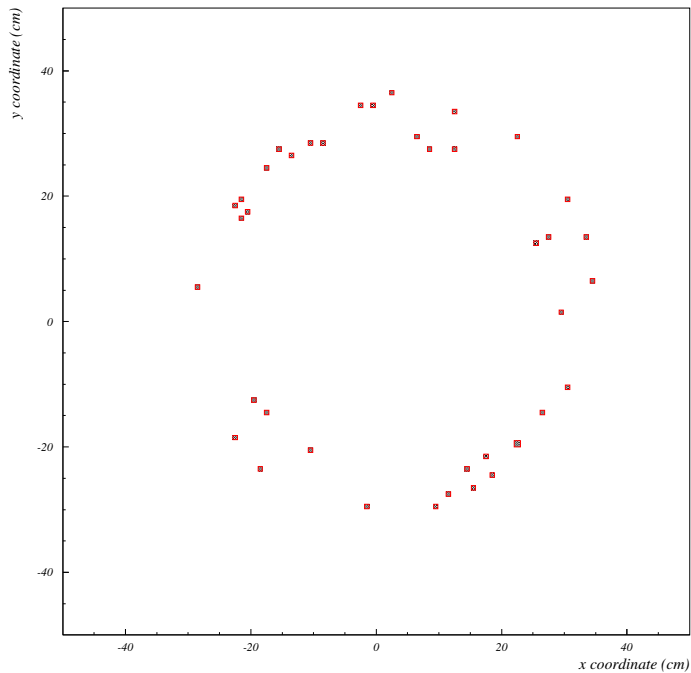


From the image on the photon detector, the Čerenkov angle of the track can be reconstructed, i.e. from the known track direction (ring center) and hit coordinate the angle is calculated and plotted:



Analysis of RICH data

Rings are accompanied by noise hits and other rings:



How to choose between the hypotheses e, μ, π, K, p ?

- 1) Count photons within $\approx 2.5\sigma$ of each hypothesis
(\rightarrow P. Abreu et al., DELPHI Coll., Phys.Lett. B334 (1994) 435)
- 2) Determine likelihood for each track and each hypothesis independently. Needed: estimates of background form, level, number of signal photons, sigma
(\rightarrow P. Baillon, Nucl. Instr. and Methods A238 (1985) 341;
P. Abreu et al., DELPHI Coll., Z. Phys. C67 (1995) 1)
- 3) Global max. likelihood: maximize likelihood for all

tracks simultaneously.

(→ R. Forty, NIM A433 (1999) 257)

4) Iterative pattern analysis: associate each photon predominately with a single track

(→ M. Starič, P.K., NIM A433 (1999) 279)

5) If only poor tracking information is available: look for rings in a stand-alone mode, use some form of Hough transform

(→ , NIM A (199))

Essential:

number of photons

single photon resolution

Summary: need about 10 for isolated, more than 20 for high density cases

Resolution of a RICH counter

Sources of error in the Č. angle measurement

- finite coordinate resolution of the photon detector

$$\sigma_{\theta} = \frac{a}{f\sqrt{12}}$$

for detector pad size a and mirror focal length f ,
e.g. $\sigma_{\theta} = 0.45$ mrad for $a = 9$ mm, $f = 5.75$ m.

- dispersion, variation of the refractive index (dn/dE) over the energy range with RMS width σ_E of detected Čerenkov photons,

$$\sigma_{\theta} = \frac{1}{\beta n^2 \sin \theta} \frac{dn}{dE} \sigma_E$$

solid radiators: 5 – 7 mrad, liquids: 3 – 4 mrad,
gases: 0.1 – 0.5 mrad (depends on the radiator and detector!).

- optical error due to the imperfections on the mirror surface and mirror misalignment, typically $\approx 0.1 - 0.2$ mrad
- finite precision in track slope parameters as determined by the tracking system

- spread in track slope parameters as caused by multiple scattering within the radiator

$$\sigma_{\theta} = \frac{1}{\sqrt{6}} 15 \text{MeV}/c \frac{\sqrt{L/X_0}}{\beta p}$$

- spread in track slope parameters due to stray magnetic fields in the radiator

$$\sigma_{\theta} = \frac{1}{\sqrt{12}} \frac{B_t L}{p} \frac{0.3 \text{GeV}/c}{T_m}$$

- the optical error due to the finite angle of incidence of photons upon the spherical mirror (spherical aberration)

In a typical case the first two dominate since they are hardest to overcome.

The combined single photon error σ_1 is a quadratic sum of the contributions.

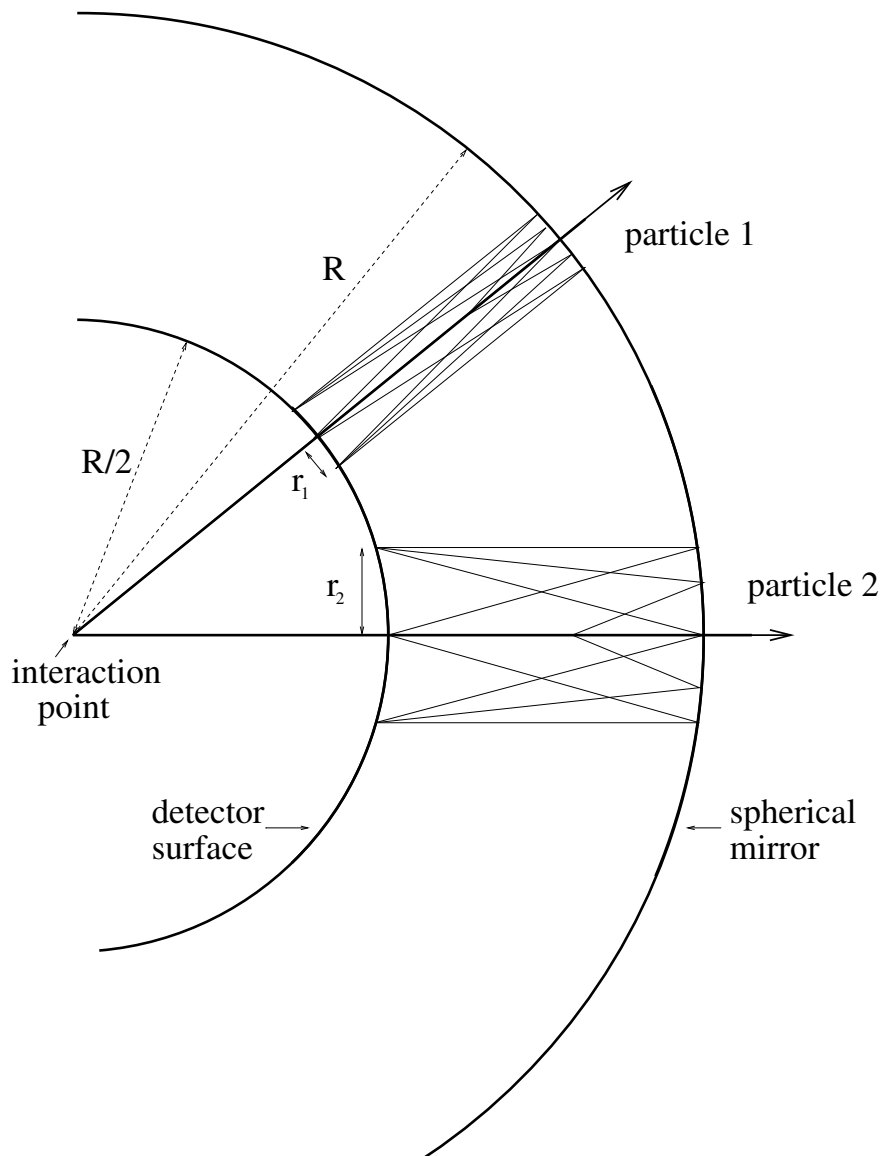
Assuming N detected photons, the overall resolution is

$$\sigma_N = \frac{\sigma_1}{\sqrt{N}}$$

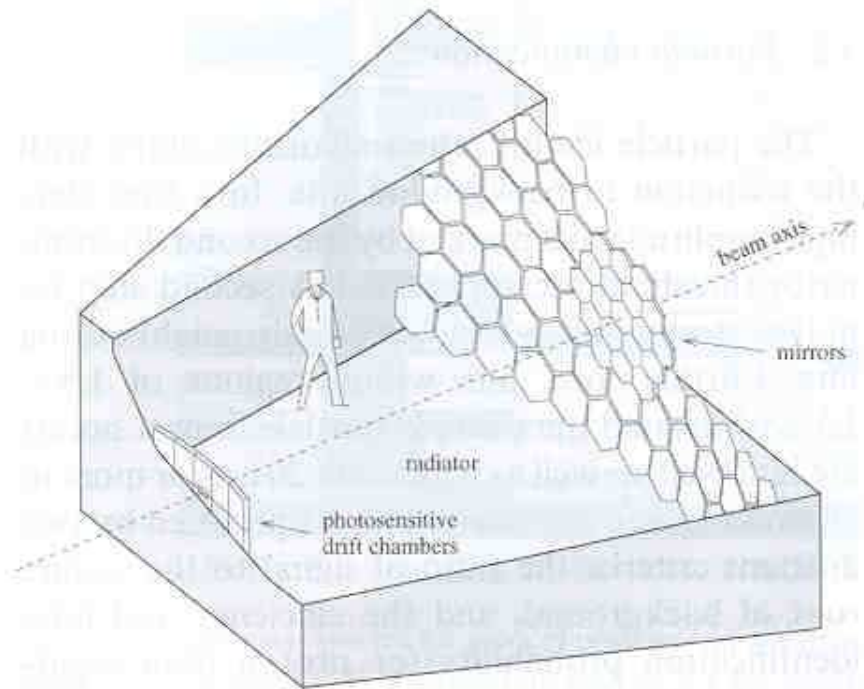
for **isolated tracks**.

RICH Designs: proximity and mirror focused

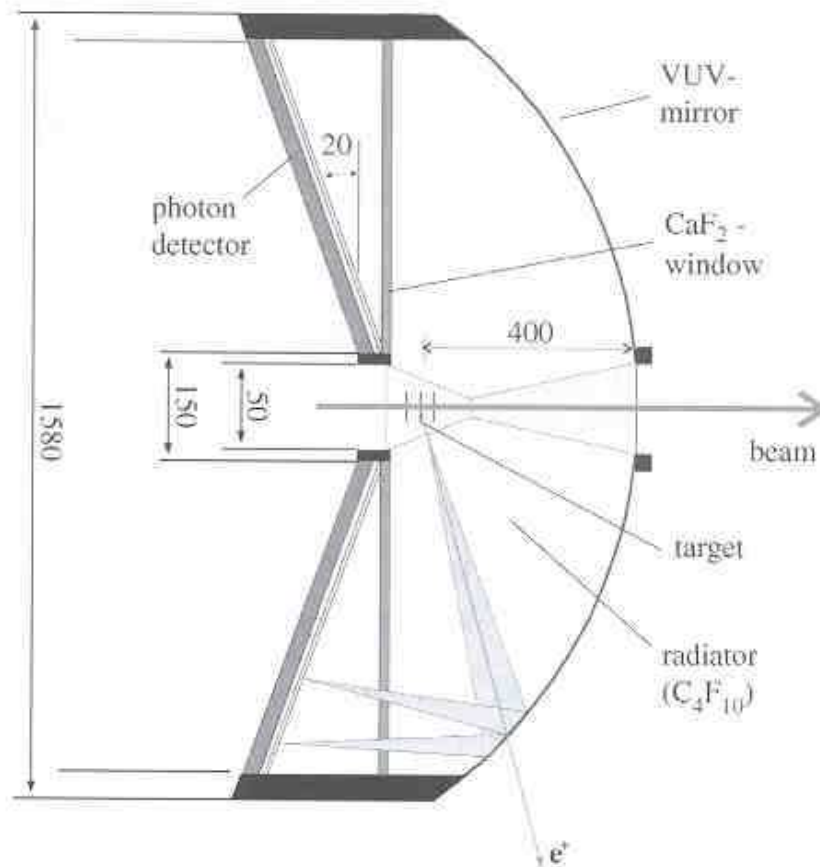
Original mirror focused



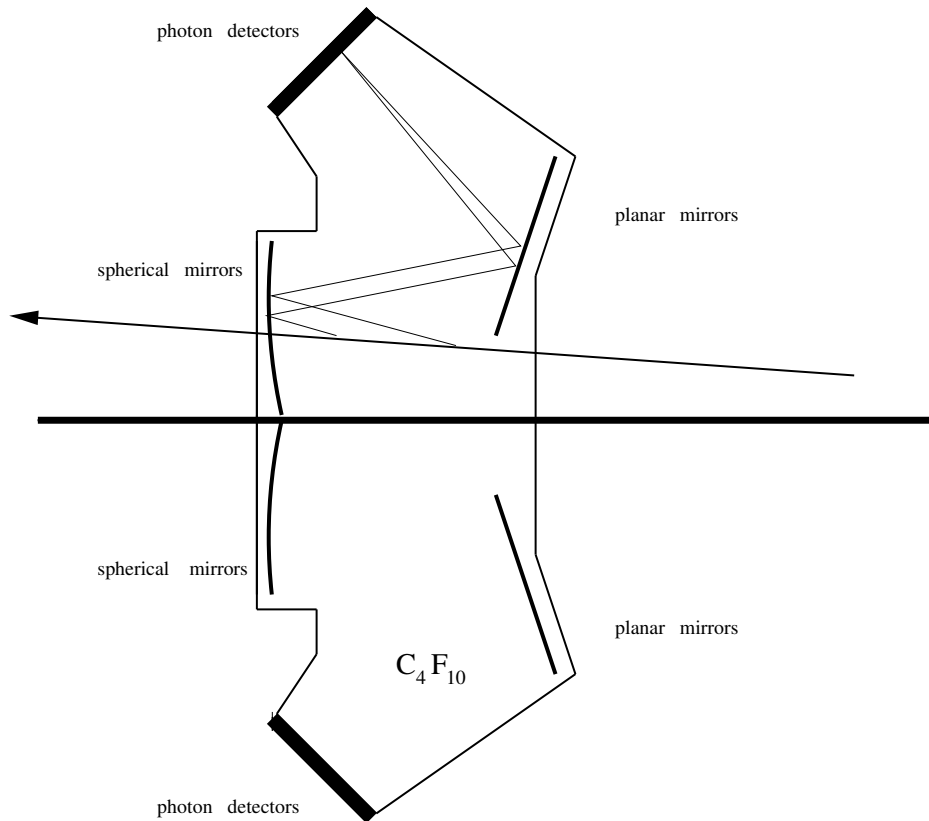
OMEGA



HADES



HERA-B



N.B. The light source is of particular nature: one has to be careful about the position, orientation, form of the photon detector plane: impact on resolution!

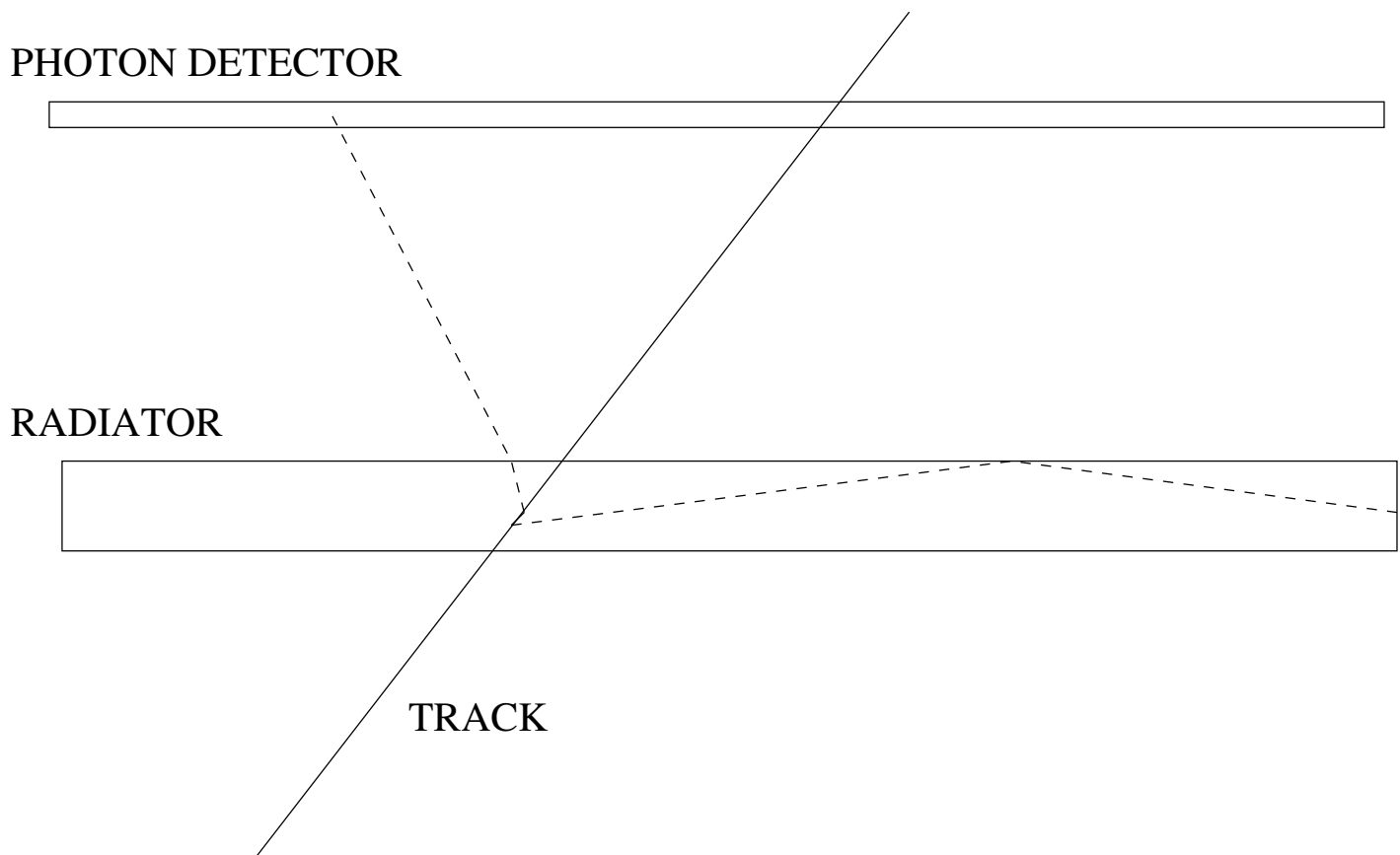
→ T. Ypsilantis, J. Seguinot, NIM **A343** (1994) 30

→ P. Križan, M. Starič, NIM **A379** (1996) 124

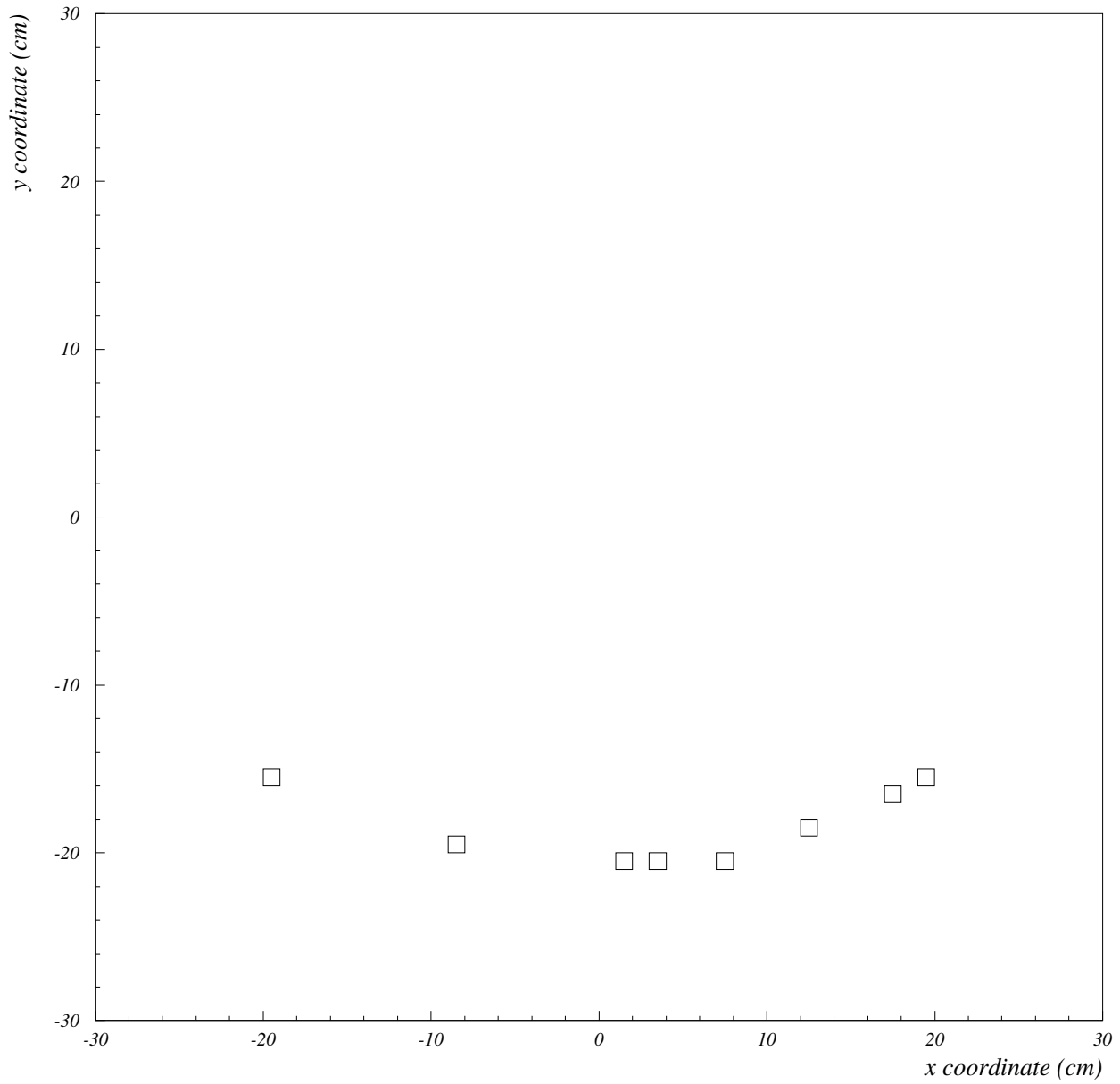
Proximity focusing RICH

Geometry variation: in case of a solid or liquid radiator, the radiator can be rather thin (only about 1 cm) - one does not need a spherical mirror.

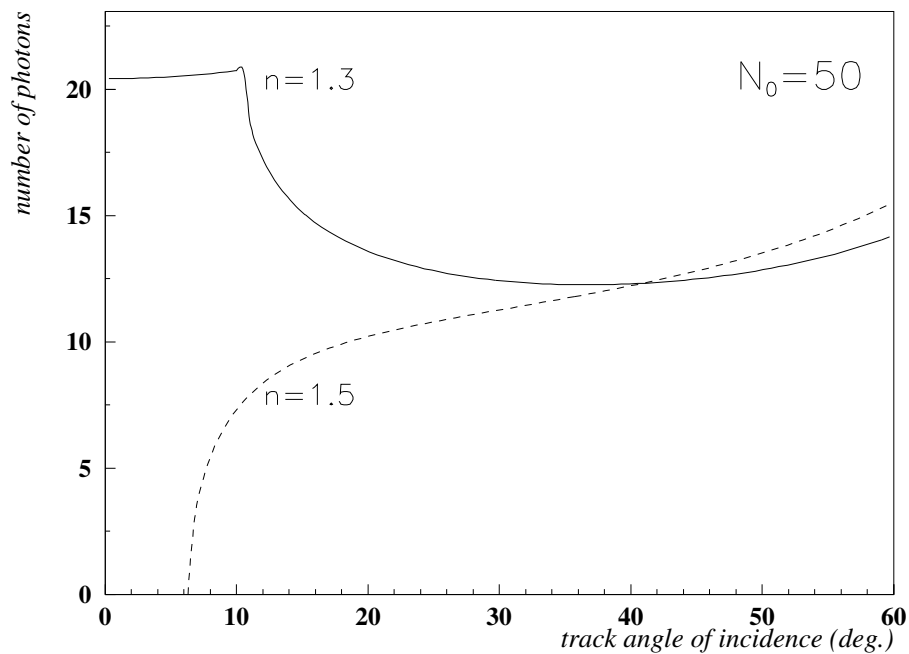
Photons are led to propagate over a distance of 10-20 cm, until they reach the photon detector.



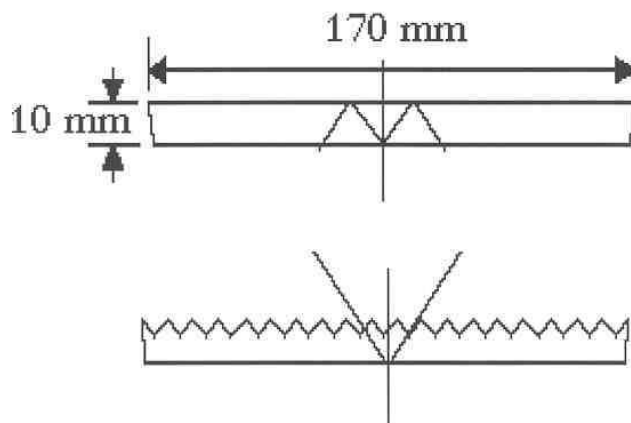
Only part of the 'ring' reaches the photon detector:



Number of detected photons depends on the angle of incidence of the track onto the radiator medium, since a sizeable fraction of photons gets trapped in the radiator by total internal reflection.

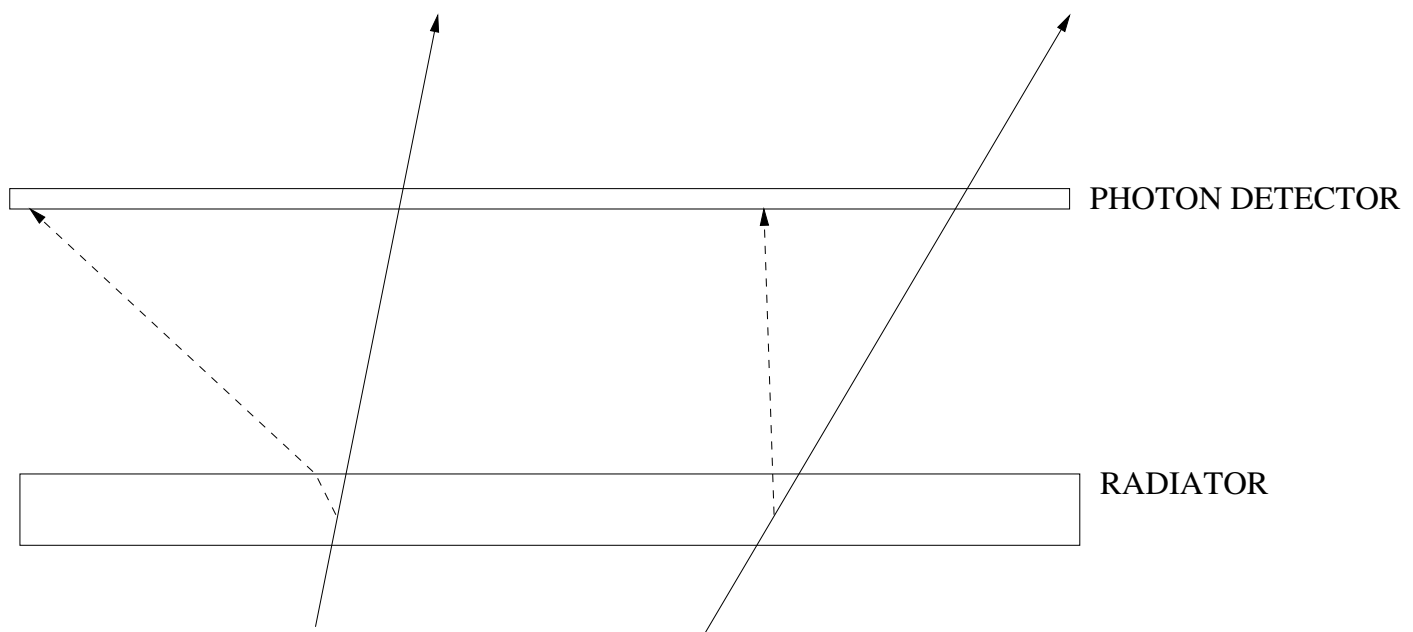


Problem with perpendicular incidence in case of $n > \sqrt{2}$: tilt the radiator or form it as a sawtooth (CLEO).



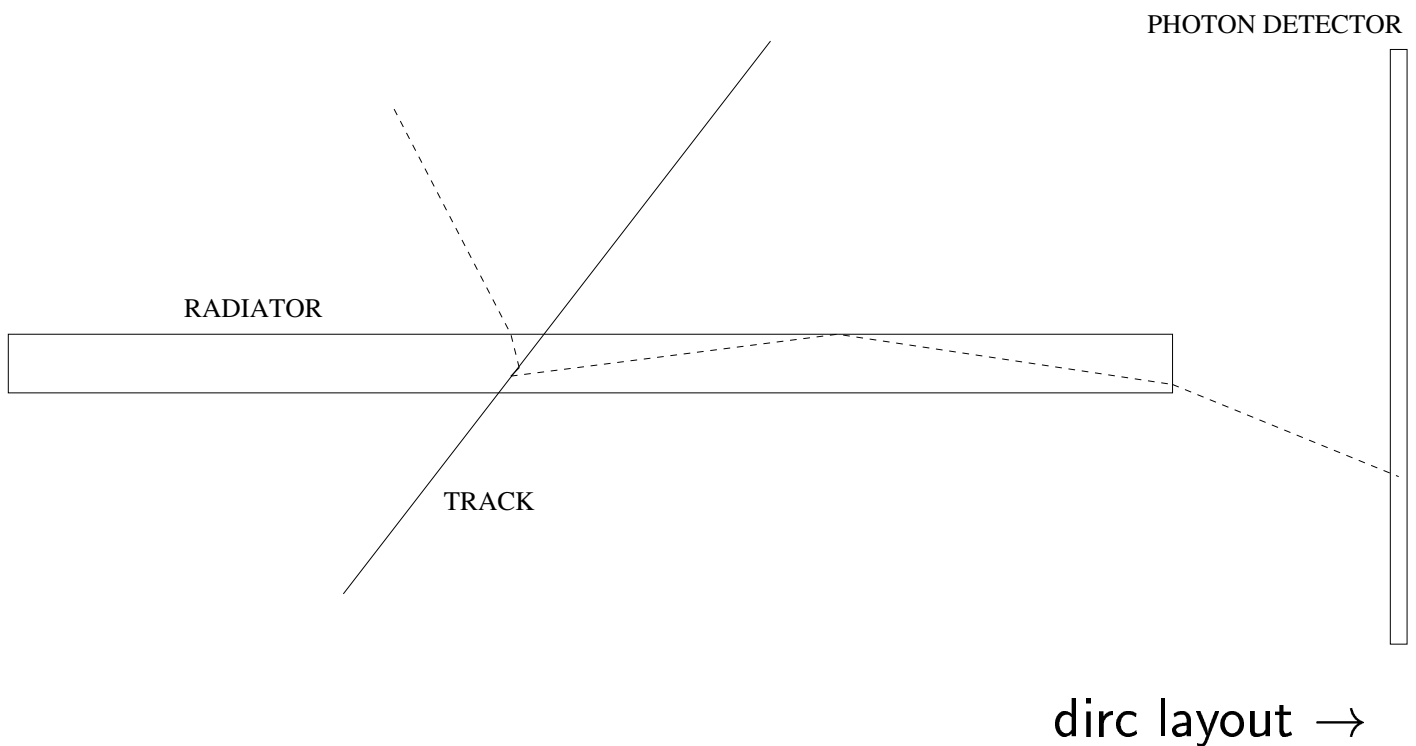
Errors in the proximity focussing case depend on the photon angle:

- detector granularity
- dispersion
- emission point error



DIRC

Geometry variation 2: photons trapped in a solid radiator are propagated along the radiator bar to the side, and detected as they exit and traverse a gap.

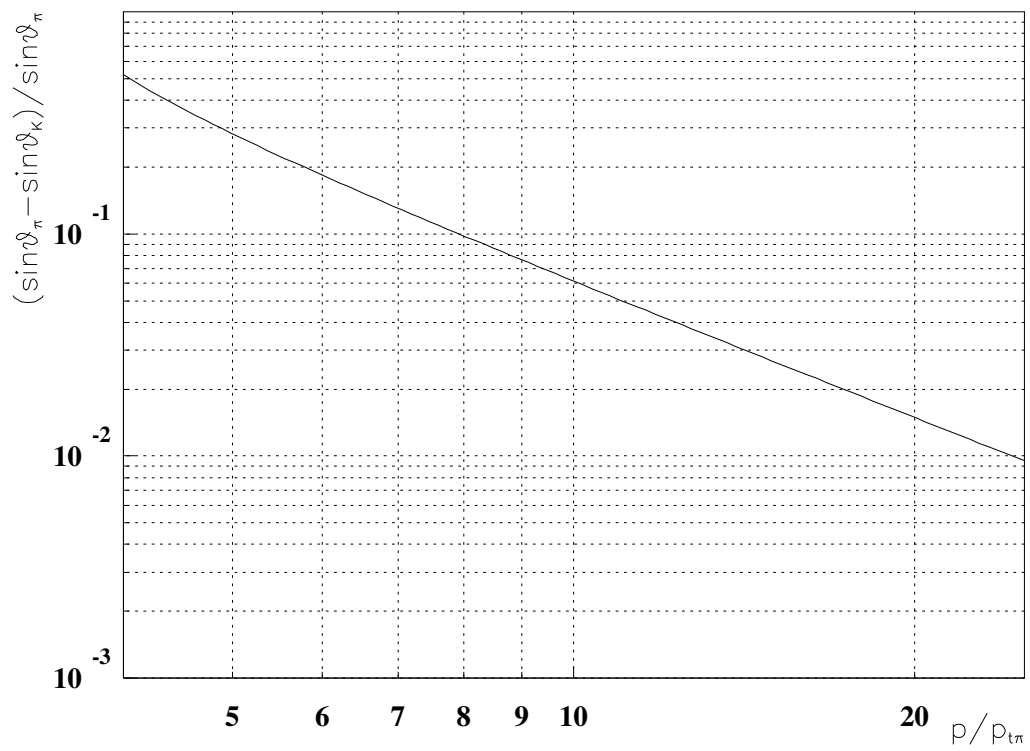
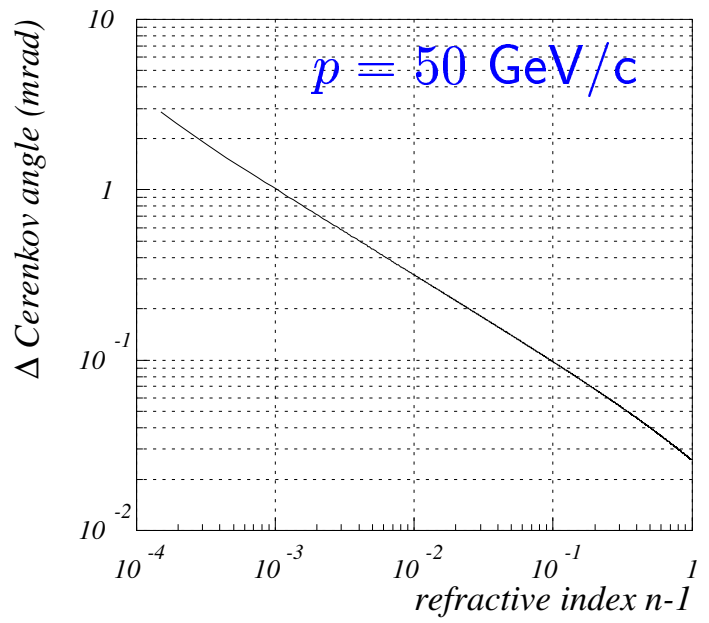
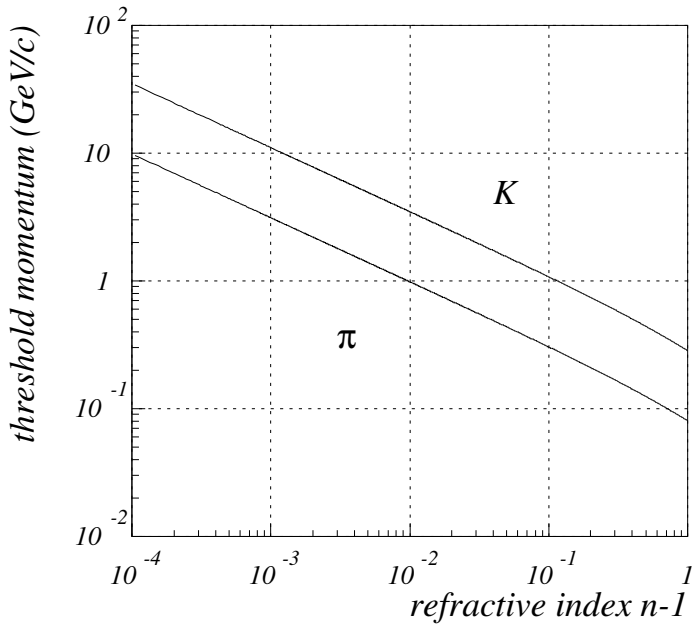


Limits of the RICH technique

The choice of RICH radiator medium in case of a specific experiment depends on the particles we would like to identify, and their kinematics:

- the threshold momentum for the lighter of the two particles we want to separate $p_t = \beta_t \gamma_t m c$, $\beta_t = 1/n$ should coincide with the lower limit of momentum spectrum p_{min} . Typically $p_{min} = \sqrt{2} p_t$.
- the resolution in Čerenkov angle should allow for a separation up to the upper limits of kinematically allowed momenta

π/K separation example:



Limiting performance at the high momentum side:
irreducible contribution to the resolution - dispersion.

radiator	LiF solid	C ₆ F ₁₄ liquid	C ₅ F ₁₂ gas	N ₂ gas	He gas
σ_θ (mrad)	7.0	3.9	0.45	0.40	0.13
σ_N (mrad)	2.2	1.2	0.14	0.13	0.04
p_{max} (GeV/c) for $3\sigma \pi/K$	3.5	6.9	50	100	330
p_{min} (GeV/c)	0.6	0.9	11	28	83

photon detector: TMAE, 10 det. photons assumed

Summary:

$$\frac{p_{max}}{p_{min}} \approx 4 - 7$$

for a 3σ separation between the two particles.

For a larger kinematic region ≥ 2 radiators are needed!

→ DELPHI, SLD (liquid+gas) →

→ HERMES (aerogel+gas)

→ LHC-b (aerogel+2 gases)

High occupancies

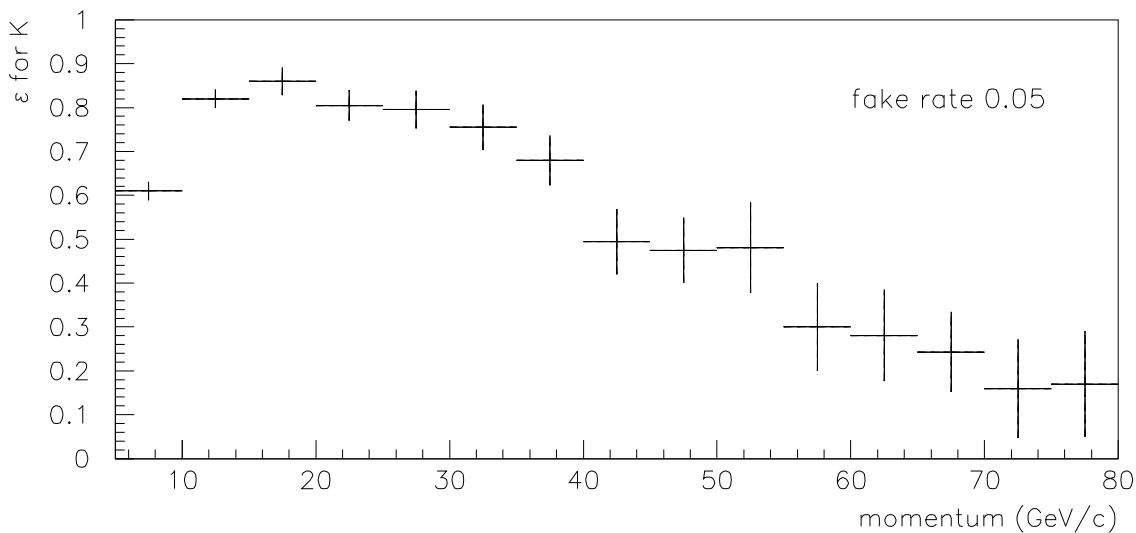
In case of a sizeable background under the Čerenkov angle peak:

effective resolution for N detected photons

$$\sigma_N > \frac{\sigma_1}{\sqrt{N}}$$

HERA-B case: for isolated rings a $3\sigma \pi/K$ separation should be possible up to $p_{max} \approx 100 \text{ GeV}/c$.

At high track densities, however, we get \rightarrow



Overview: RICH Building Blocks

Need 10 - 20 detected photons and a good angular resolution:

how do we get there?

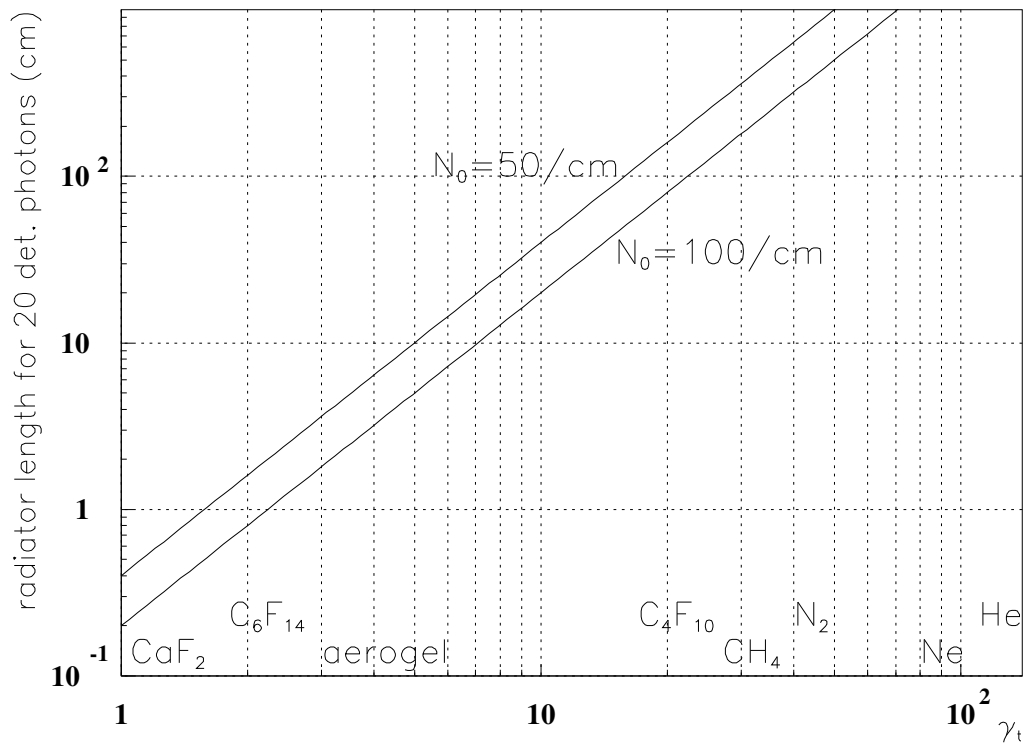
Very carefully design, build and run a RICH counter

RICH Building Blocks

- Radiators
- Photon detectors
- Light collectors
- Large system aspects

Radiators

Radiator length needed for 20 detected photons in case of $\beta = 1$ particles



Photon detectors

Need:

- photosensitive substance
- amplification/multiplication of the photoelectron

Photosensitive substances:

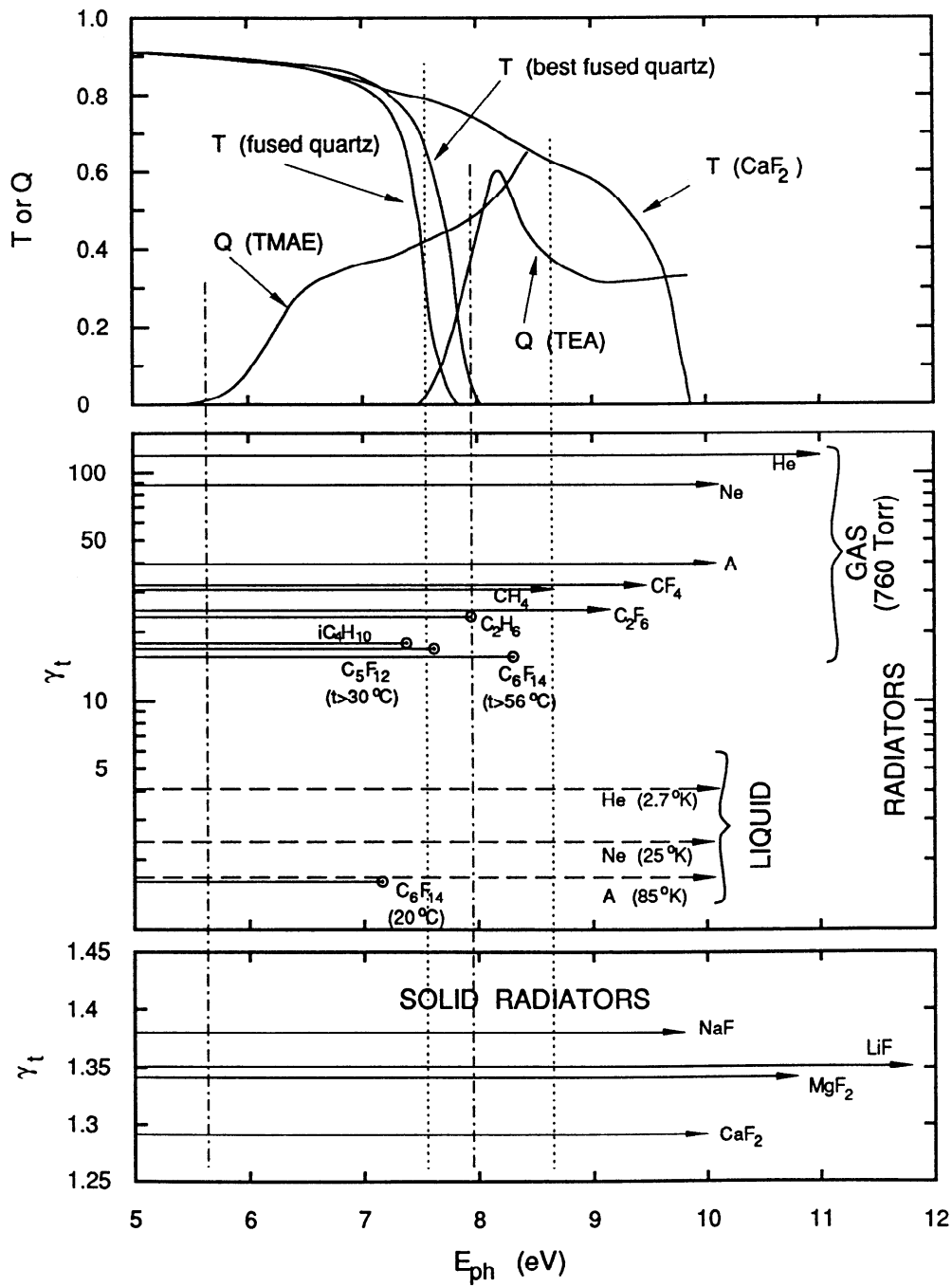
- solids (SbCs, Sb-K-Cs, CsI, ...)
- gases (TMAE, TEA)

Multiplication through:

- multiplication in a dynode structure in vacuum
- avalanche amplification in a gas
- avalanche amplification in silicon
- photoelectron acceleration in electric field in vacuum, detection in Si

Combined to:

- gas based photon detectors (wire chambers with 2d read-out)
- vacuum based photon detectors (PMTs, HPDs)
- silicon based photon detectors (APD, VLPC)



Detection efficiency/radiator transmission windows.

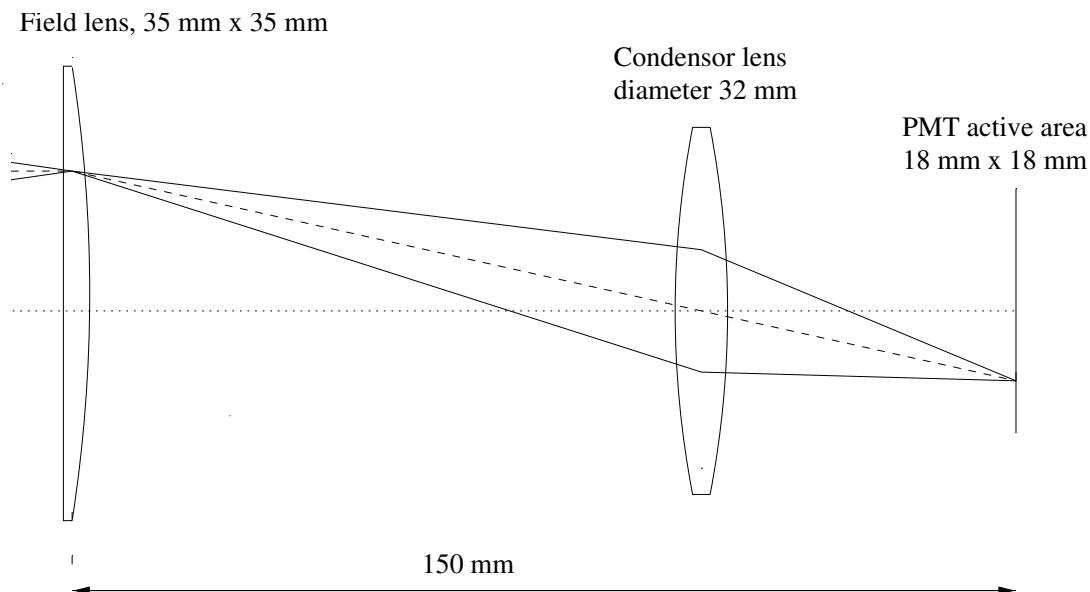
Light collectors

are used to reduce the dead area between photon detector segments (in particular in the case of PMTs), or to adapt the required photon detector granularity to the PMT (pad) size

Winston cones

reflectors

lens combinations



Example: Optical system for light collection and demagnification of the HERA-B RICH.

→ **angular acceptance, material transmission**

Mirrors

Good reflectivity in UV: not trivial to produce and maintain (water!).

But: was done and worked very well (DELPHI RICH, SLD CRID) for years

DELPHI mirror system →

HERA-B mirror system →

Typically: 0.5-1 cm of glass, coated with Al, and a protective layer (MgF_2 etc).

Light mirrors: on composite substrate (expensive!)

Windows

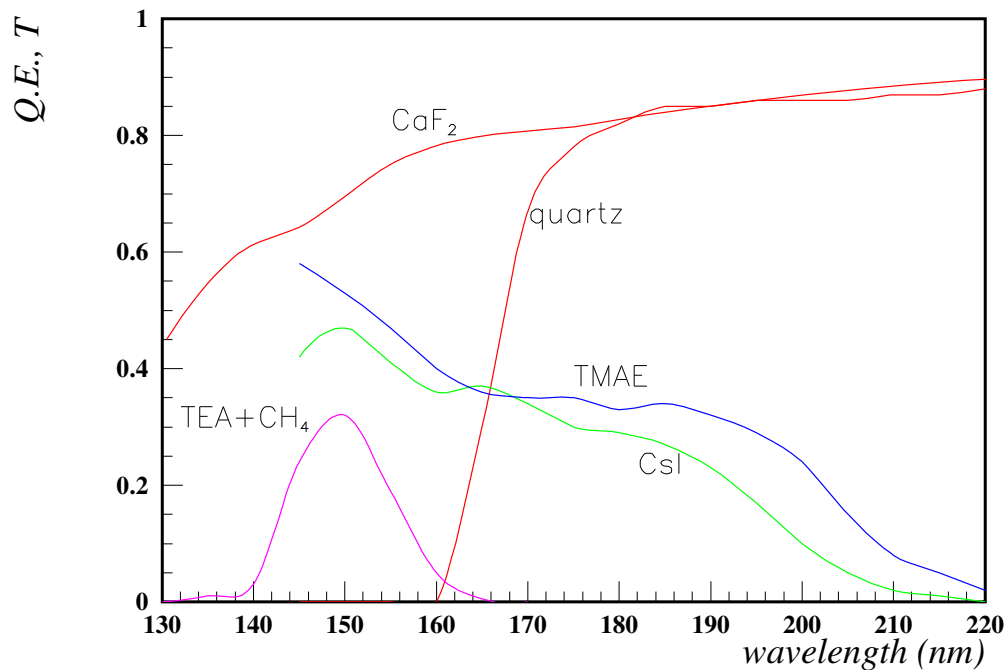
Transmission of radiator exit windows has to match the sensitivity of the photosensitive substance.

quartz for TMAE, CsI

CaF₂ for TEA

UVT plexiglass for PMTs

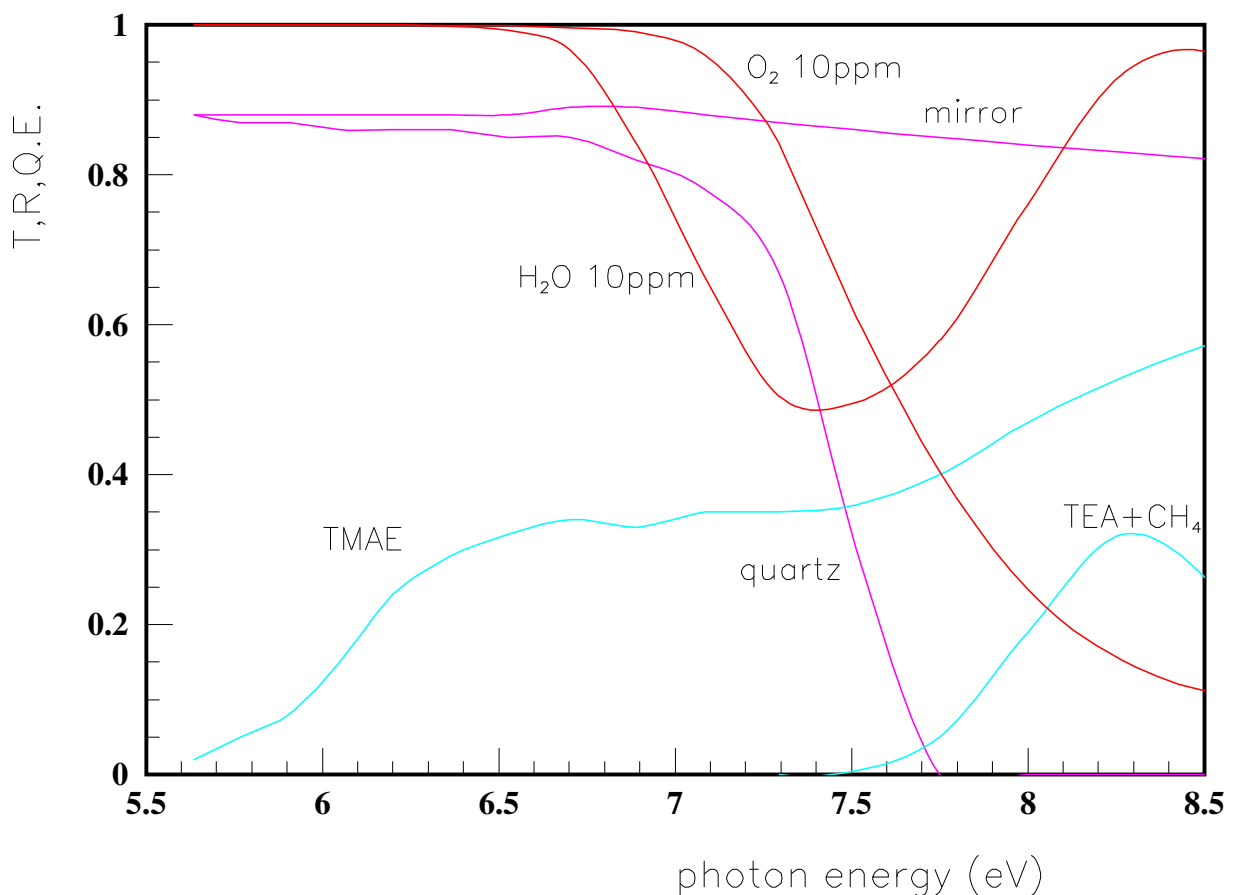
For comparison: mylar is only transparent above ≈ 400 nm, UVT plexiglass above 300 nm.



Large system aspects

Water and oxygen content in the radiator (order of one meter to a few meters of gas, or a centimeter of liquid) have to be kept very low in case of photon detectors for UV light.

Example: take a RICH with average photon path of 7.5 m (0.75 m), plot the influence of 10 ppm (100 ppm) of water or oxygen.



Short historical excursion

1934 Čerenkov characterizes the radiation

1938 Frank, Tamm give the theoretical explanation

50-ties - 70-ties Čerenkov counters are developed and are being used in nuclear and particle physics experiments, as differential and threshold counters

1977 Ypsilantis, Seguinot introduce the idea of a RICH counter with a large area wire chamber based photon detector

1981-83 first use of a RICH counter in a particle physics experiment (E605)

1992→ first results from the DELPHI RICH, SLD CRID, OMEGA RICH

Gas based detectors (TMAE, TEA, CsI)

Why bother to develop gas chamber based light sensitive detectors instead of photomultiplier tubes?

Virtues:

- good spatial resolution (order few mm),
- coverage of large surfaces (square meters) with a large fraction of active area at reasonable cost,
- highly efficient single photon detection.

These virtues made gas based detectors boost the RICH identification method.

Single photon detection in wire chambers

Wire chambers detect charged particles. To detect a photon, one has to make sure it reacts with the chamber material, walls or gas, and produces a photoelectron, which is then detected in the chamber.

A well known example: detection of X-rays in a MWPC with an argon-methane gas mixture.

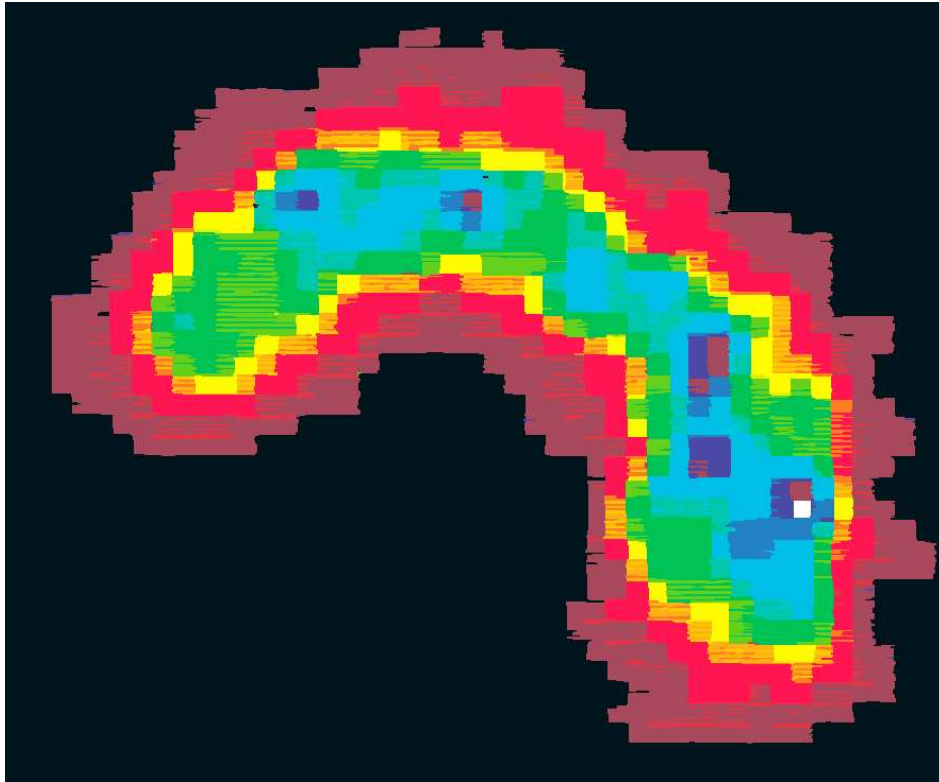
Can one detect UV or visual photons as well?

In principle yes, however

- a photosensitive material is needed that survives in the chamber gas mixture (PMTs have vacuum inside!)
- the photoelectron produced has a very low energy, so that it does not make any more primary electron-ion pairs - the avalanche is started by a single electron.

Example: metal surface

Note that a polished metal surface is sensitive to visual light, although with a very low efficiency.



The photograph of the tungsten filament in a light bulb was taken with a small 5cm x 5cm MWPC with a two dimensional delay line read-out, the object was projected onto the cathode plane through a small hole in a black box (*camera obscura*).

From: M. Starič et al., NIM **A323** (1992) 91-96

Photosensitive materials

To get a reasonable efficiency, order 10%-20%, one has to use quite special materials.

They are typically chemically active, so that care has to be taken on how they are handled, and how clean the inside of the chamber is.

- Photosensitive gas additives

TEA Tri Ethyl Amine

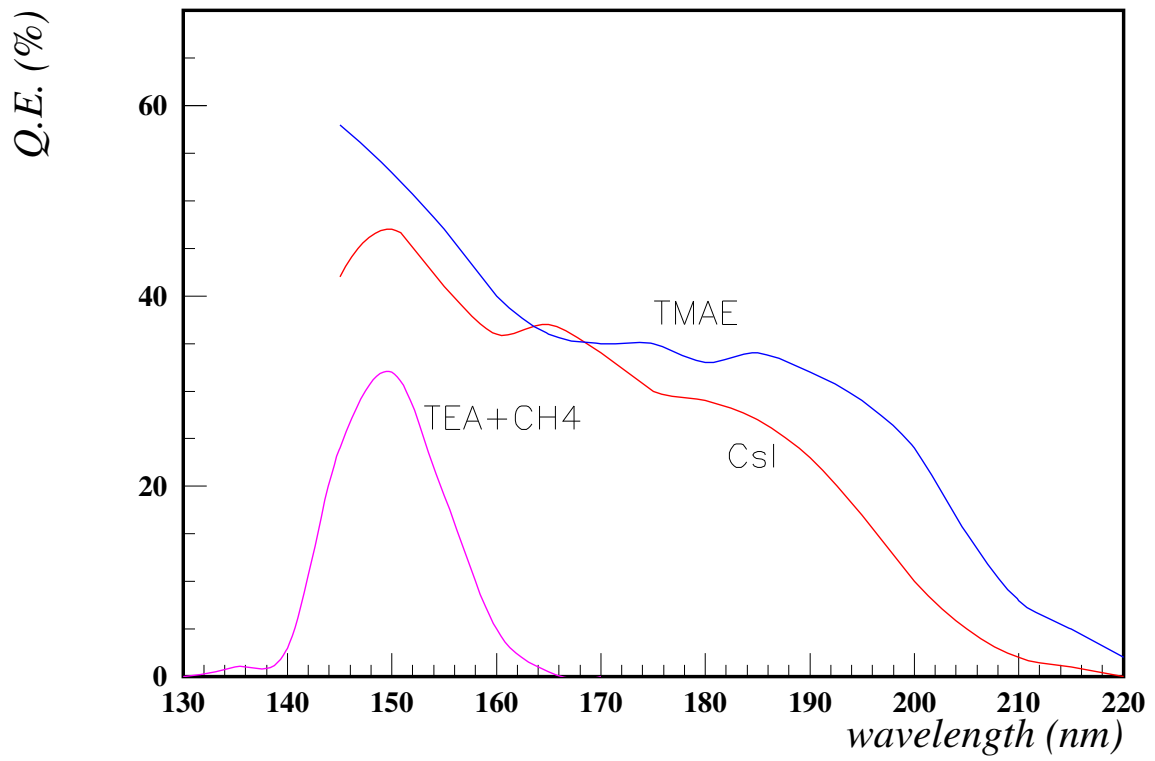
TMAE Tetrakis diMethyl Amino Ethylene

- Solid photosensitive layers on the read-out cathode or entrance window

CsI

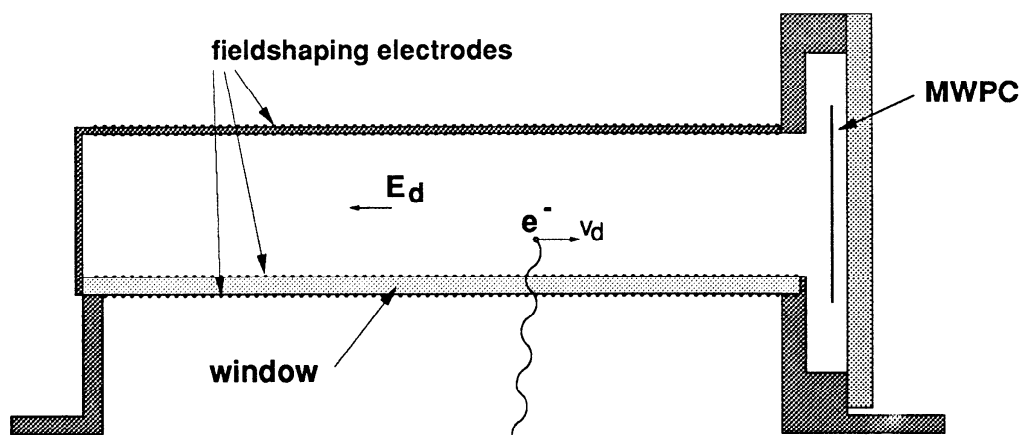
new materials e.g. K-Cs-Sb, coated with CsI or

CsBr: sensitive in visual, still under study



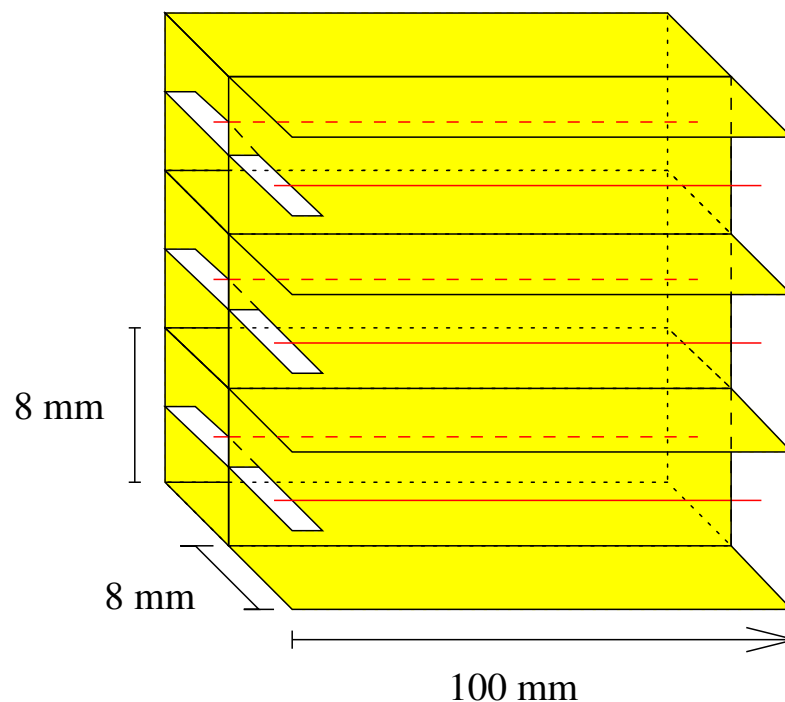
TMAE

- A liquid at room temperature, with a vapour pressure of 0.30 torr (at 20⁰C) and the absorption cross section $\sigma_{UV} = 30Mb$.
- Absorption length of about 3 cm at room temperature.
- Typical chamber: a thick conversion volume (≈ 10 cm) is needed to enable an efficient absorption, usually combined with a TPC type chamber.



- Gas purity: very clean system needed (TMAE reacts intensely with oxygen!), stainless steel pipes and valves, oxysorb.
- Chamber materials: TMAE reacts with most common chamber materials.

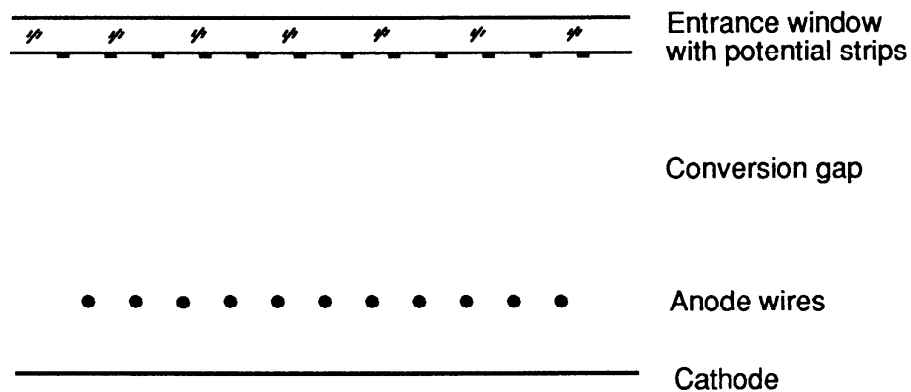
- Examples:
 - * TPC (Omega, DELPHI, SLD)
 - * multiwire chamber with pad read-out (Caprice)
 - * two parallel plate stages, coupled to a multiwire chamber with pad read-out (CERES)
 - * egg-crate structure (JETSET)
- Higher rates: a different geometry is needed. An example is the JETSET/HERA-B prototype geometry with anode wires embedded in an egg-crate structure.



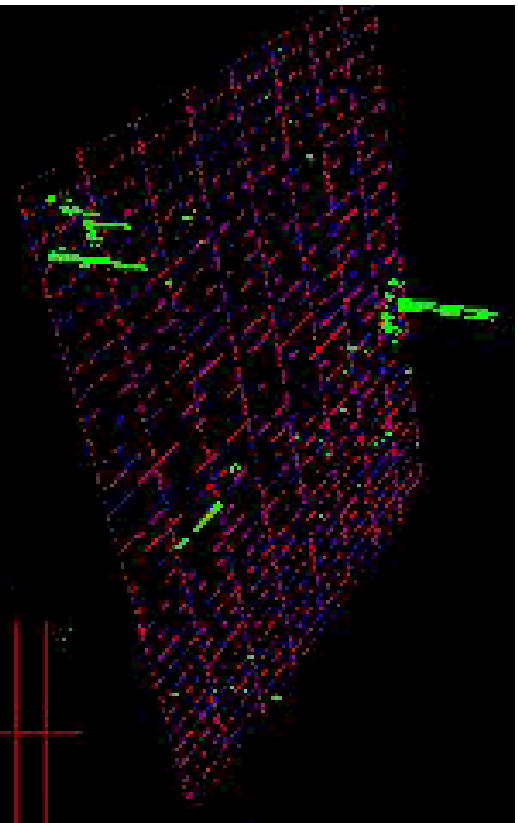
Photons enter the chamber from the left side.

TEA

- A liquid at room temperature, with a vapour pressure of 52 torr (at 20⁰C) and the absorption cross section $\sigma_{UV} = 10Mb$.
- Absorption length of 0.61mm (at 20⁰C).
- Typical chamber: a multiwire chamber with pad read-out.

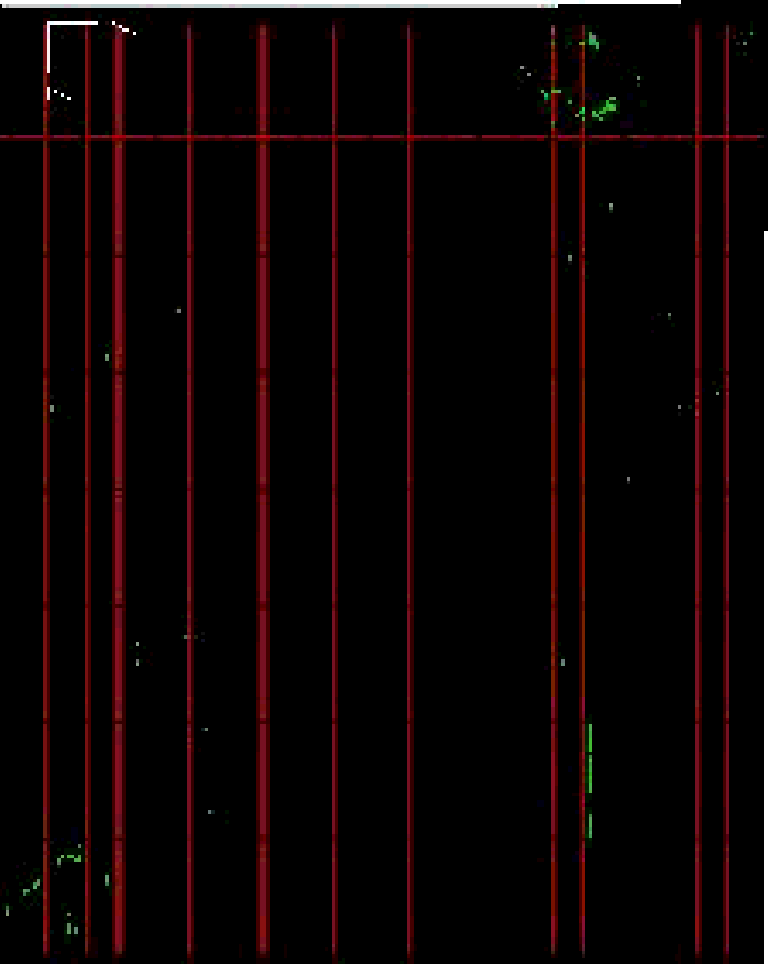


- Typical dimensions: few mm thick.
- First used in the pioneering RICH experiment E605.
- Examples: multiwire chamber with pad read-out (College de France, CLEO III)



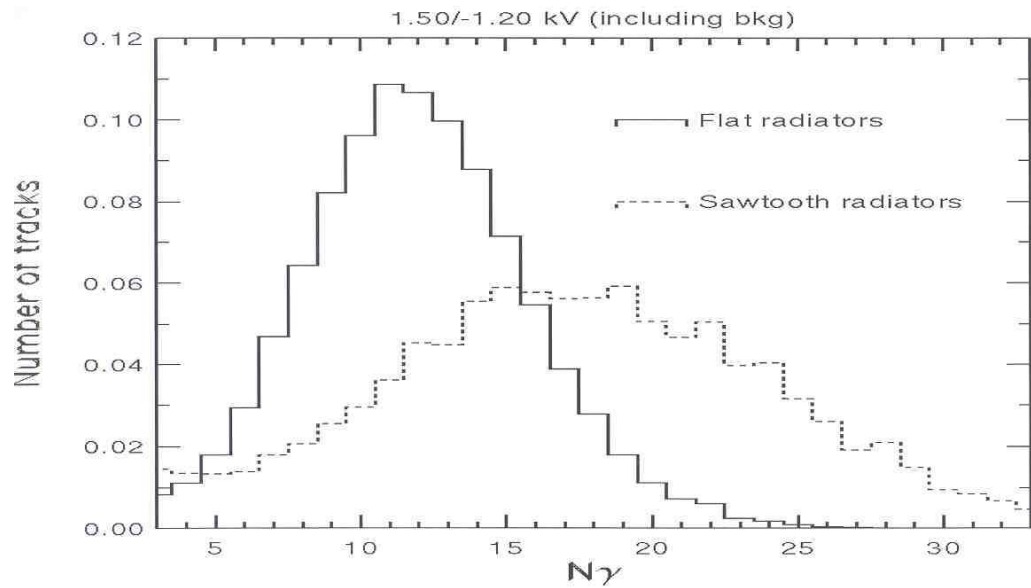
Plane Radiator

Bhabha Event

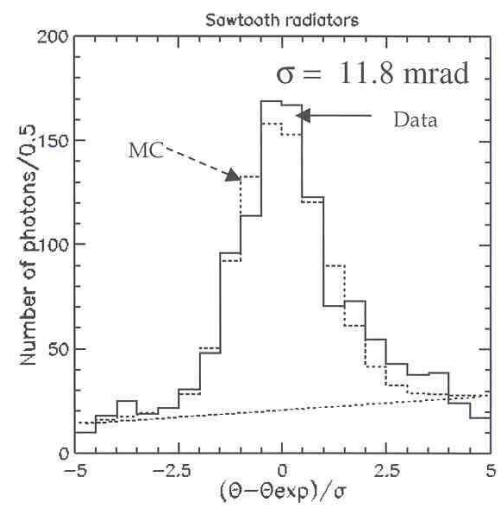
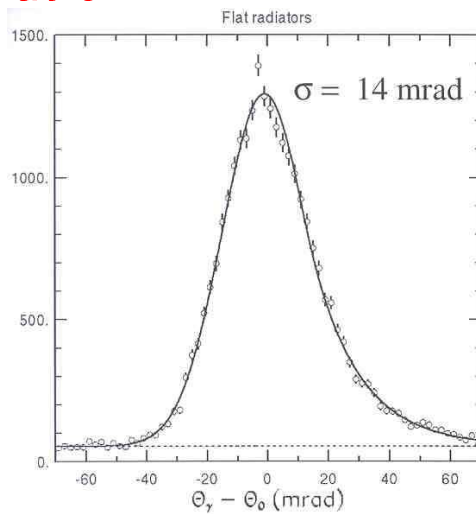


CLEO III RICH: presently under commissioning,
excellent test results!

Number of detected photons

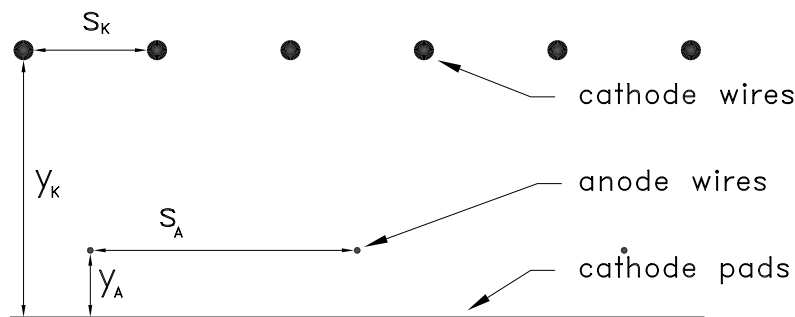


Resolution





- A solid layer, 100nm - 1 μ m thick, evaporated on one of the cathodes (or on the entrance window).
- Needs a high purity chamber gas, usually methane with a water and oxygen content of order ppm.
- Typical chamber: a multiwire chamber with pad read-out, reflective photocathode.

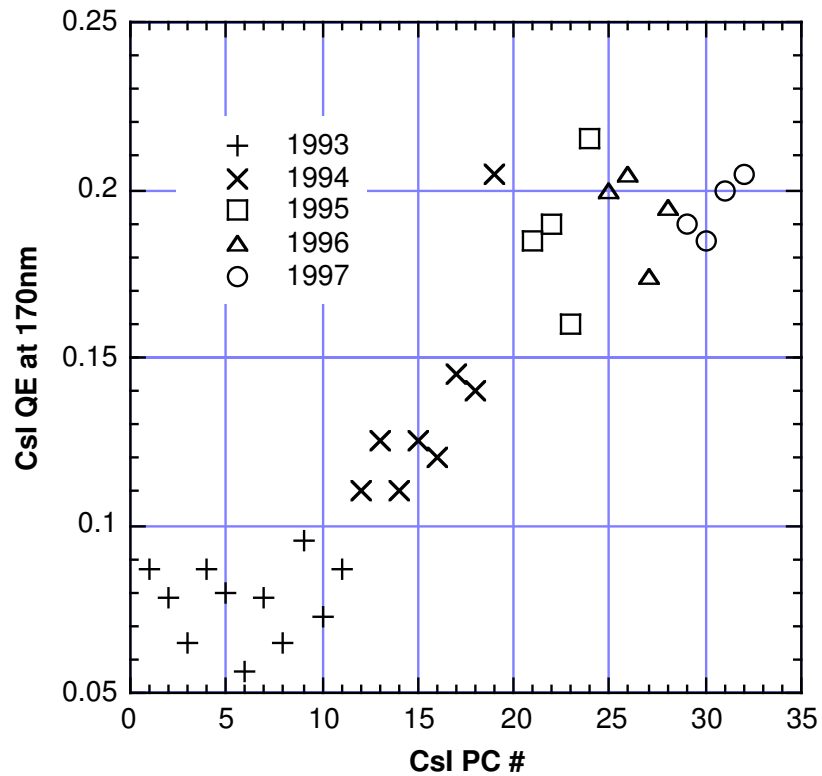


- Electric field: voltage on cathode wires has to be adjusted to guarantee a uniform amplification around the anode wire.
- Chamber variation: photocathode evaporated on the entry window, chamber can then be a MSGC, MGC, can also have a GEM amplification structure and multiwire chamber with pad read-out.

CsI cathode handling

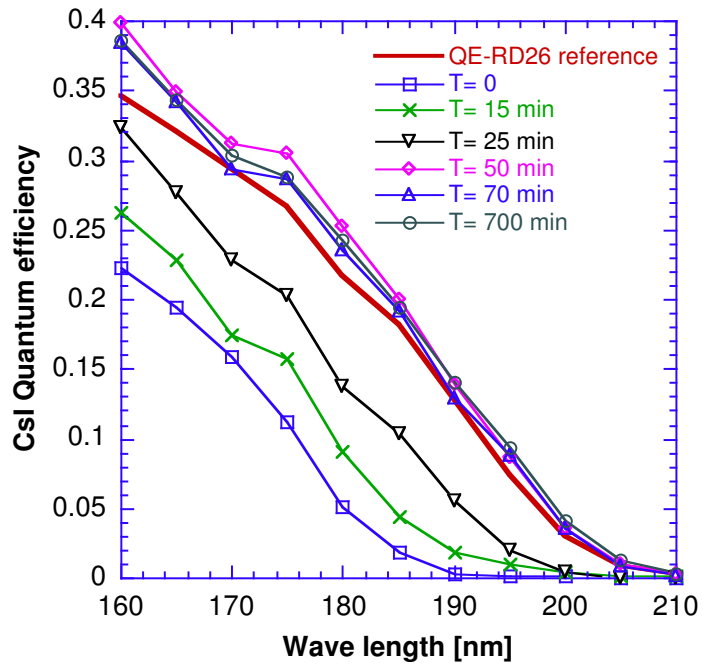
A lot of progress in R+D over the past few years:

- learning curve: Q.E. vs. t, RD-26

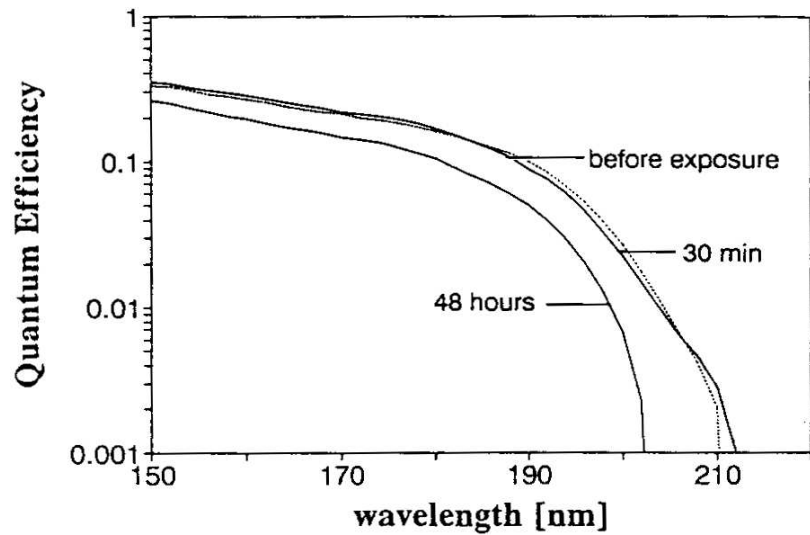


- influence of substrate material (→ photo)

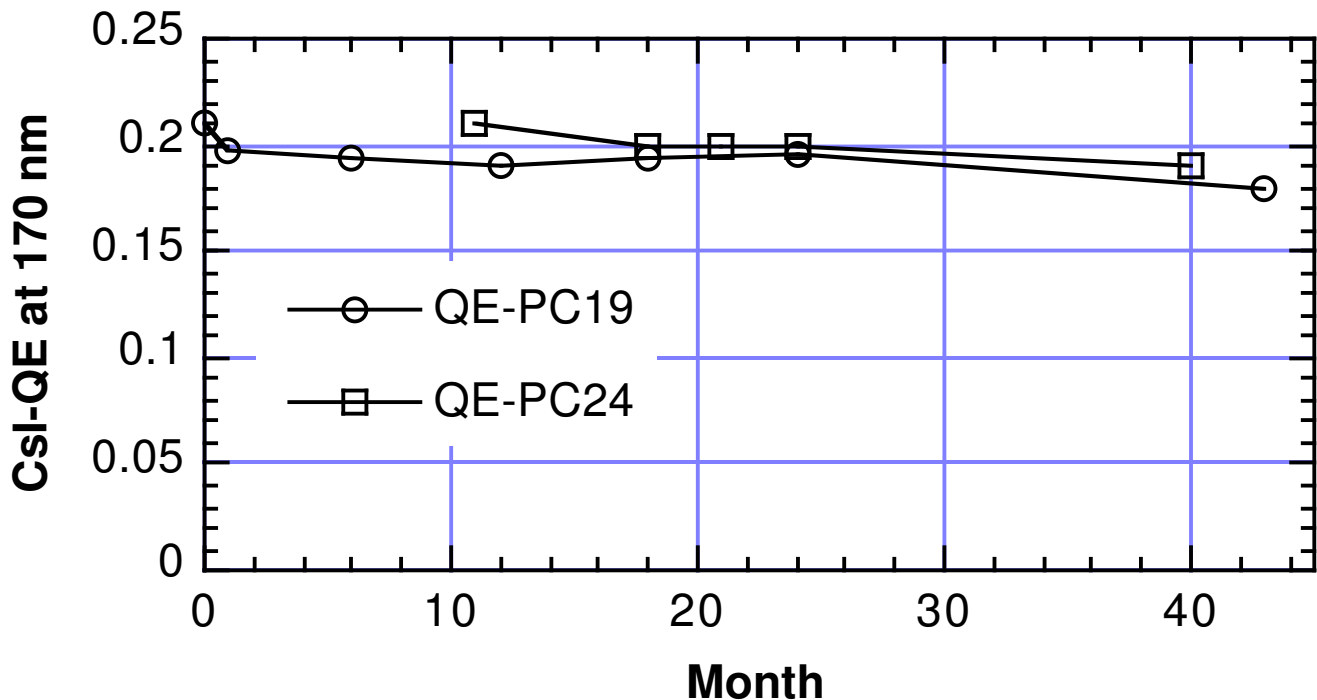
- influence of initial conditioning: keeping for several hours at 60 C in vacuum



- exposure to air: should not exceed 1/2 hour



□ stability in the chamber

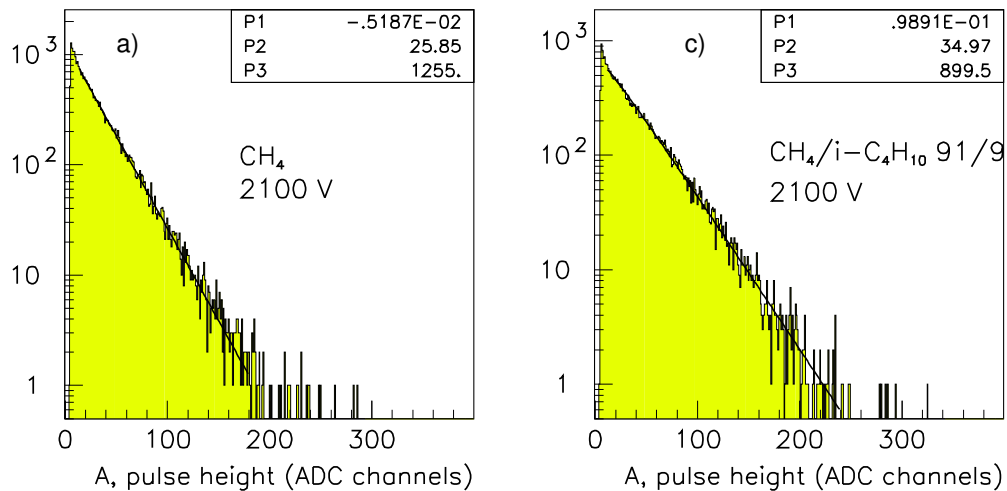


Examples:

- multiwire chamber with pad read-out (College de France/CERN, RD26 - CERN, RD26 - Saclay, HADES prototype (TU Munich), HERA-B prototype, Princeton, Compass prototype)
- MSGC and MGC (HADES prototype, Weizmann, Pisa) with a transmissive photocathode
- chamber with a GEM preamplification stage (Weizmann)

Single primary electron pulse height

A typical pulse height spectrum of single electrons has the exponential shape with a large fraction of low pulses (see Appendix B).



Only at high gains ($> 10^5$) the distribution flattens off at low gain, or even peaks at a nonzero value.

Single primary electron detection

For the exponential pulse height distribution,

$$\frac{dw}{dU} = \frac{1}{\bar{U}} e^{-U/\bar{U}},$$

the single electron detection efficiency amounts to

$$\epsilon = \int_{U_{th}}^{\infty} \frac{dw}{dU} dU = e^{-U_{th}/\bar{U}}$$

for the pulse height threshold set to U_{th} .

For a highly efficient photoelectron detector we clearly need low noise electronics (small U_{th}).

The **visual charge** is only about **20%** (for integration times of order 20ns) of the avalanche charge, i.e. at a gas amplification of $2 \cdot 10^5$ the average detected signal corresponds to $4 \cdot 10^4$ electrons. If we want to cut noise at 4σ , and keep a **90%** efficiency ($U_{th} = 0.1\bar{U}$), the electronics noise has to be kept at

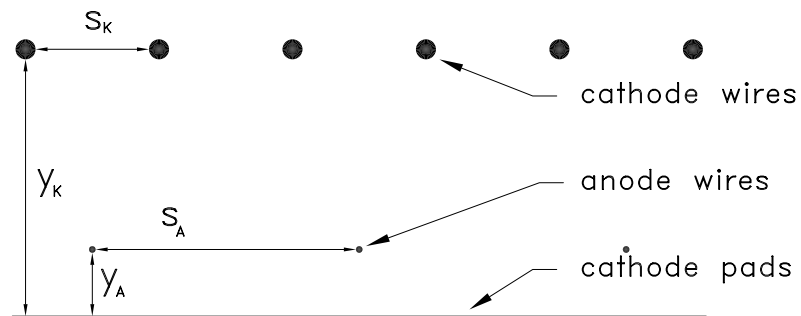
$$\frac{2 \cdot 10^5 \cdot 0.2 \cdot 0.1}{4} = 1000 e^- ENC$$

Problems of wire chamber based photon detectors

feedback photons

anode related effects

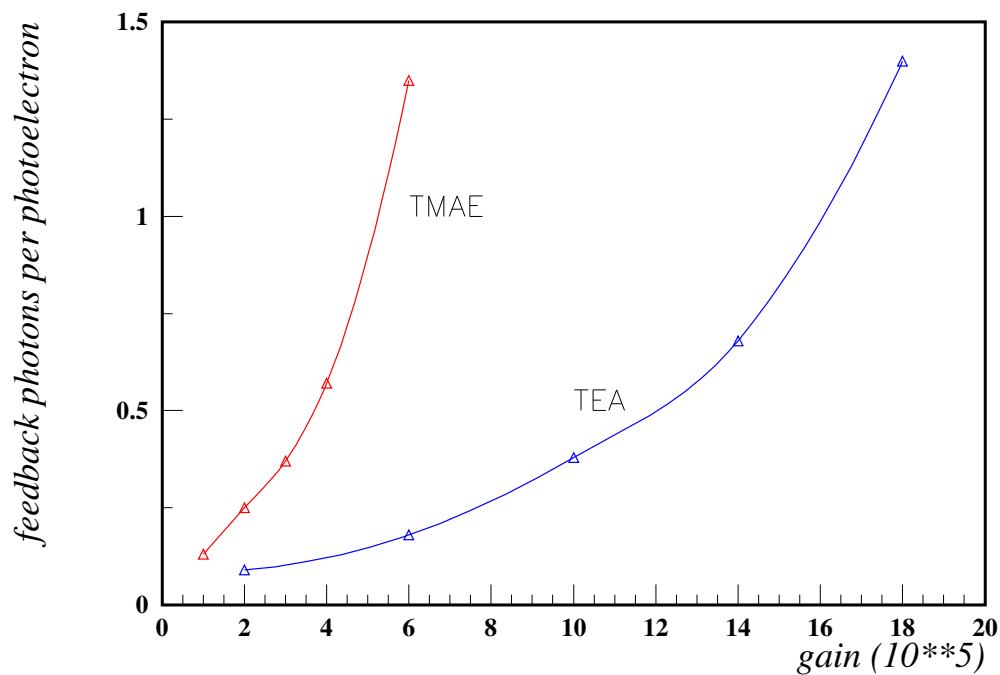
cathode related effects



Feedback photons

Avalanche photons cause emission of secondary photons (feedback photons). The process is enhanced because

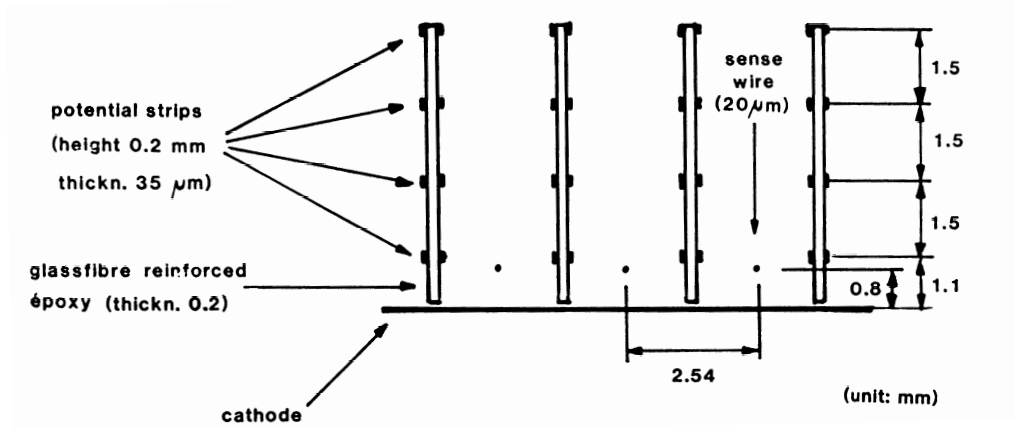
- chamber is light sensitive
- no or little quenching gas is used



The result is more background (best case) or chamber instability (in particular in cases when a lot of primary electrons are liberated by a charged track which passed the chamber).

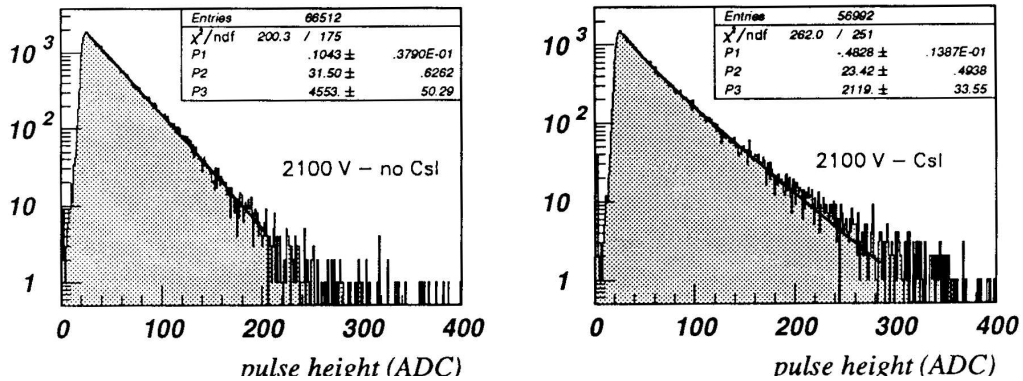
Solution:

- use **isolated cell** geometry a la JETSET (see above) or
- **isolate anode wires** from each other by using blinds, or



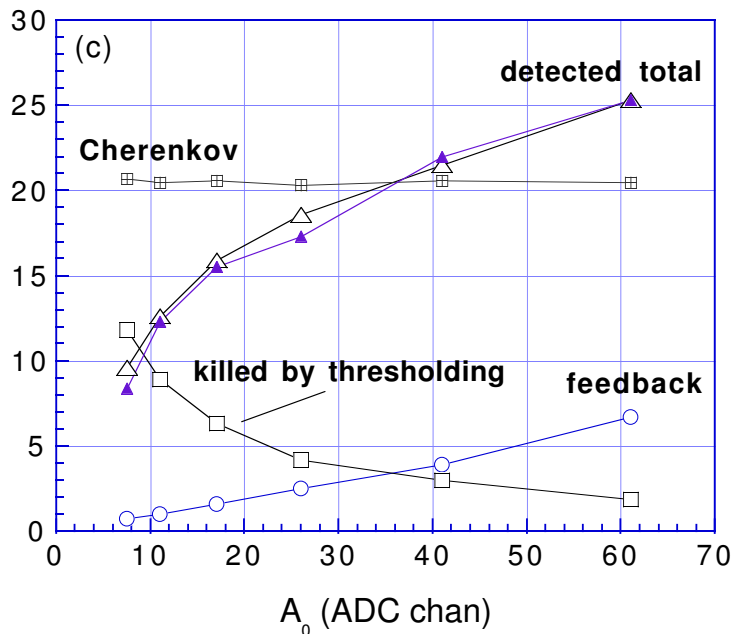
- work at **low gain**, preferably in a region with **no charged tracks**.

Feedback photons in CsI chambers



- could be dangerous: open geometry
- less problematic: thin gas volume
- working point: gas amplification is a compromise between detection efficiency and cluster size and overlap, detector occupancy.

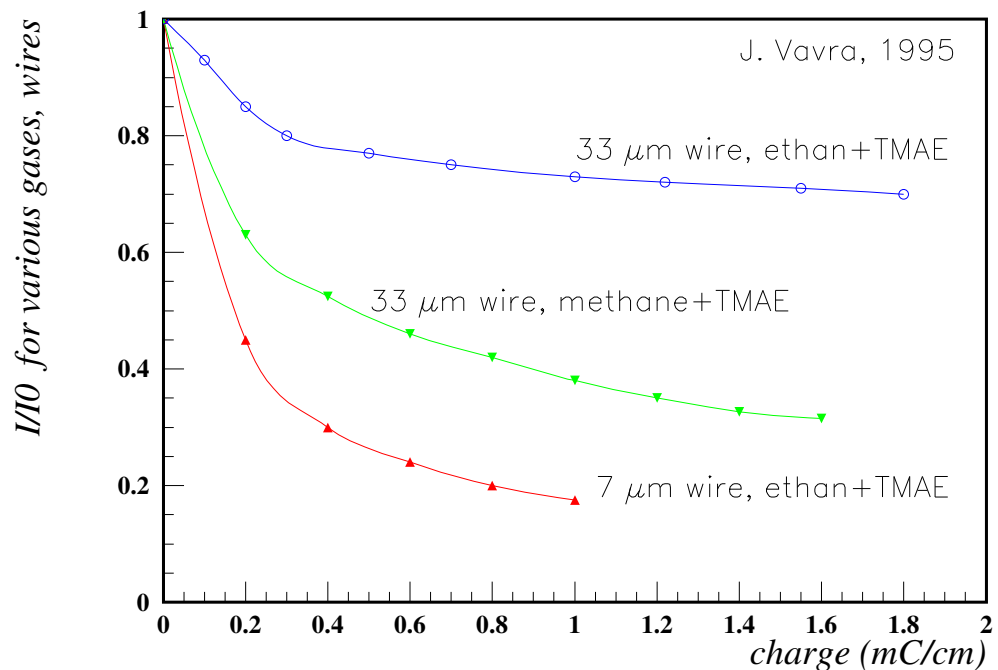
RD-26 study: number of detected photoelectrons vs. average pulse height



Anode wire ageing

Cause: accumulation of polymerisation deposits on the anode wires, particularly in TMAE loaded gases.

Consequence: gas amplification drops as a function of deposited charge.



→ J. Vavra et al., NIM **A367** (1995) 353

→ HERA-B study: J. Pyrlík et al., NIM **A433** (1999) 92

A drop of amplification by a factor k decreases the efficiency to

$$\epsilon' = e^{-U_{th}/\bar{U}'} = e^{-\frac{U_{th}}{\bar{U}/k}} = \epsilon^k,$$

from 90% detection efficiency it drops to 50% after

an amplification drop by a factor of 6, and from 80% we arrive at 50% already after a drop by a factor 3.

Recovery?

Increase high voltage (a rise by 200 V increases the gas amplification by about a factor of 2.4 in a methane filled chamber with $20\mu m$ anode wires), but this clearly cannot be carried out too many times if we already start with an operating voltage of 2400 V, in particular for cases where the irradiation is not uniform over the chamber.

Remove deposits by washing the wires with alcohols, or heating.

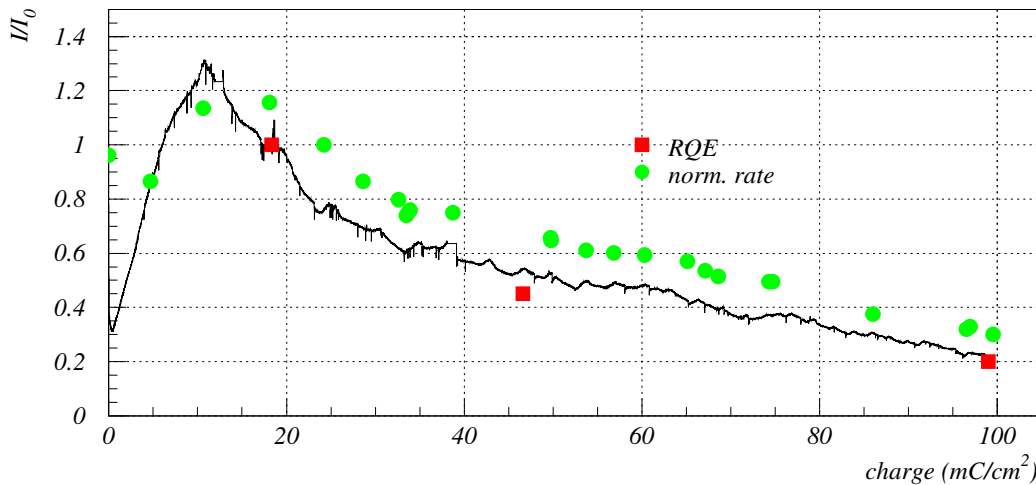
SLD CRID pioneered the heating by using carbon wires (high resistivity). → J. Va' vra et al., IEEE Trans. Nucl. Sci. 45 (1998) 648.

Attractive: *in situ* heatable anode wires for high rate applications, e.g. as studied for the HERA-B prototype → D. Škrk et al., IEEE Trans. Nucl. Sci. 46 (1999) 317

Cathode related effects

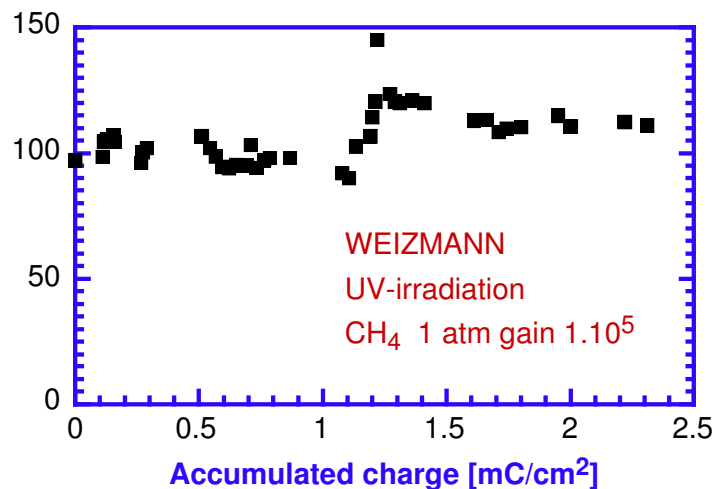
- TMAE: Accumulation of polymerisation deposits on the cathode planes (typically good insulators) can cause a large electric field after enough charge has accumulated, making possible the emission of electrons from the cathode - **Malter effect**. This, in turn, can cause periodic bursts of charge - observed in the SLD CRID → J. Va'vra, NIM A367 (1995) 353-357.
Remedy? As a possibility adding water (at tens of ppm level) was proposed, with the idea that it would help in the same way it does in drift chambers (cathode conductivity).

- **Csl: Photocathode ageing:** decay of the Csl layer during the recombination of ions from the avalanches.



An example of Csl ageing: note the initial drop, 1 to 0.3. → HERA-B RICH group, NIM **A387** (1997) 146

Is Csl ageing less pronounced at lower rates?



Ageing effects were also reported at high photon fluxes even without gas amplification.

Remedy? Protective covers were tried - little success.

→ Make the chamber in such a way that the photo-cathode (backplane of the chamber) can be easily exchanged.

Summary on RICHes with wire chamber based photon detectors

- Only UV photons can be detected, their detection is not trivial.
- However: large system have been successfully operated for years.
- A new generation of experiments is under commissioning or construction.
- Visual photon detection in gas chambers: being developed.
- High rate operation: problematic, in particular if long term stability is required - more R+D needed to become competitive with PMTs.

More on the subject:

1. Čerenkov counters: overview
 - J. Seguinot and T. Ypsilantis, A historical survey of ring imaging Cherenkov counters, NIM **A343** (1996) 1-29.
 - T. Ypsilantis and J. Seguinot, Theory of ring imaging Cherenkov counters, NIM **A343** (1996) 30-51.
2. Čerenkov counters: status
 - Proceedings of the First Workshop on Ring Imaging Cherenkov Detectors - Experimental Techniques of Cherenkov Light Imaging, Bari, Italy, June 2-5, 1993, NIM **A343** (1996).
 - Proceedings of RICH '95: International Workshop on RICH Counters, Uppsala, Sweden, June 12 - 16, 1995, NIM **A371** (1996).
 - Proceedings of RICH '98: Ein Gedi, Israel, Nov. 15 - 21, 1998, NIM **A433** (1999).
3. UV photon detection: overviews
 - J. Va'vra, Photon detectors, NIM **A371** (1996) 33-56.
 - A. Breskin, CsI UV photocathodes: history and mystery, NIM **A371** (1996) 116-136.
 - F. Piuz et al., ALICE HMPID, CERN/LHCC 98-19.
4. avalanche development, pulse height statistics
 - P. Rice-Evans, Spark, streamer, proportional and drift chambers, Richelieu, London (1974)
 - F. Sauli, Principles of operation of multiwire proportional and drift chambers, in Experimental techniques in High-Energy Nuclear and Particle Physics, T. Ferbel (editor), World Scientific (1991)

Appendix A: derivation of

$\frac{d\sigma}{d(\hbar\omega)}$ a la Allison, Cobb

- Solve Maxwell's Equations with charge density

$$\rho = e_0 \delta^3(\vec{r} - \vec{\beta}ct) \text{ and current density } \vec{j} = \vec{\beta}c\rho \rightarrow$$

$$\phi(\vec{k}, \omega) = \frac{e_0}{2\pi\epsilon\epsilon_0 k^2} \delta(\omega - \vec{k} \cdot \vec{\beta}c)$$

$$\vec{A}(\vec{k}, \omega) = \frac{e_0}{2\pi\epsilon_0 c^2} \frac{(\omega\vec{k}/k^2 - \vec{\beta}c)}{(\epsilon\omega^2/c^2 - k^2)} \delta(\omega - \vec{k} \cdot \vec{\beta}c)$$

$$\rightarrow \vec{E}(\vec{r}, t) =$$

$$\frac{1}{(2\pi)^2} \int \int [i\omega\vec{A}(\vec{k}, \omega) - i\vec{k}\phi(\vec{k}, \omega)] e^{i(\vec{k} \cdot \vec{r} - \omega t)} d^3k d\omega \quad (\text{A1})$$

- The energy loss is due to the component of this electric field in the direction β doing work on the particle at the point $\vec{r} = \vec{\beta}ct$:

$$\langle \frac{dE}{dx} \rangle = \frac{e_0}{\beta} \vec{E}(\vec{\beta}ct, t) \cdot \vec{\beta} \quad (\text{A2})$$

- The energy loss is re-written as a probability of energy transfers

$$\langle \frac{dE}{dx} \rangle =$$

$$- \int_0^\infty d(\hbar\omega) \int_{\frac{\hbar\omega}{\beta c}}^\infty d(\hbar k) n_e \hbar\omega \frac{d^2\sigma}{d(\hbar\omega)d(\hbar k)} \quad (\text{A3})$$

where n_e is the electron density and $\frac{d^2\sigma}{d(\hbar\omega)d(\hbar k)}$ is the double differential cross section per electron.

Comparing (A1) and (A2) with (A3) we derive

$$\frac{d^2\sigma}{d(\hbar\omega)d(\hbar k)} = \frac{e_0^2}{4\pi\epsilon_0} \frac{2}{n_e \pi \hbar^2 \beta^2} \left[p \left(\beta^2 - \frac{E^2}{p^2 c^2} \right) m \frac{1}{(\epsilon E^2 - p^2 c^2)} - \frac{1}{pc^2} m \frac{1}{\epsilon} \right]$$

This formula already shows the $1/\beta^2$ factor which dominates the rate of energy loss at non relativistic velocities.

- Determine the complex function $\epsilon(k, \omega) = \epsilon_1 + i\epsilon_2$
 - photoabsorption from cross-section $\sigma_\gamma(\hbar\omega)$ and sum rules $\rightarrow \epsilon_2$ for on mass-shell photons ($\omega = kc$),
 - the Kramers-Kronig relation $\rightarrow \epsilon_1$ in terms of ϵ_2 ,
 - the dipole approximation \rightarrow for small k $\epsilon(k, \omega)$ is independent of k at fixed ω ,
 - constituent scattering from quasi-free electrons and the Bethe sum rule $\rightarrow \epsilon$ in the large k off-mass-shell region.

- Integrate the cross section over momentum transfer

$$\begin{aligned} \frac{d\sigma}{d(\hbar\omega)} &= \frac{\alpha}{\beta^2 \pi} \frac{\sigma_\gamma(\hbar\omega)}{\hbar\omega Z} \log \left[(1 - \beta^2 \epsilon_1)^2 + \beta^4 \epsilon_2^2 \right]^{-\frac{1}{2}} \\ &+ \frac{\alpha}{\beta^2 \pi} \frac{\sigma_\gamma(\hbar\omega)}{\hbar\omega Z} \log \left[\frac{2mc^2 \beta^2}{\hbar\omega} \right] \\ &+ \frac{\alpha}{\beta^2 \pi} \frac{1}{n_e \hbar c} \left[\beta^2 - \frac{\epsilon_1}{|\epsilon|^2} \right] \Theta \\ &+ \frac{\alpha}{\beta^2 \pi} \frac{1}{(\hbar\omega)^2} \int_0^{\hbar\omega} \frac{\sigma_\gamma(\hbar\omega')}{Z} d(\hbar\omega') \end{aligned}$$

where $\alpha = \frac{e^2}{4\pi\epsilon_0 \hbar c}$ is the fine structure constant, ϵ_1 and ϵ_2 are the real and imaginary parts of the on-mass-shell dielectric constant and

Θ is the phase of $1 - \epsilon_1\beta^2 + i\epsilon_2\beta^2$.

Comments:

First term has a factor $\log(1 - \beta^2\epsilon_1)$, responsible for the relativistic rise of the energy-loss cross section and its saturation.

Third term: in the optical region σ_γ vanishes and only the second term contributes \rightarrow Čerenkov radiation.

Phase: $\Theta = 0$ below, and π above threshold. We get the familiar formula for the number of emitted photons per unit track path length and photon energy interval $\frac{d^2N}{d(\hbar\omega)dx} = \frac{\alpha}{\hbar c} \left[1 - \frac{1}{\beta^2\epsilon}\right]$

When ϵ_2 and σ_γ do not vanish, the separate interpretation of this term in the cross section dissolves and it may even be negative.

Last term: constituent scattering from electrons. It is a Rutherford scattering term, shows no relativistic behaviour and is the only non-zero term for energy transfers $\hbar\omega$ in the far X-ray region, describes δ -ray production.

Appendix B: Statistics of the avalanche caused by a single primary electron

Avalanche multiplication is described by the multiplication coefficient α (also first Townsend coefficient). The mean free path between ionizing collisions is $1/\alpha$, and for a case of constant field on average $e^{\alpha x}$ electrons are produced in an avalanche over a distance x .

The fluctuations are, however, large, in particular due to fluctuations in the number of ionisations in the initial part of the avalanche.

The distribution over the number of electrons produced in the avalanche is derived as follows.

The probability that an electron ionizes an atom to produce a new electron is equal to

$$\alpha dx$$

Starting with one electron we ask what is the probability $P(n, x)$ that n electrons will result at a distance x ?

The probabilities have to satisfy a set of differential equations

$$\frac{d}{dx}P(1, x) = -\alpha P(1, x)$$

$$\frac{d}{dx}P(2, x) = -2\alpha P(2, x) + \alpha P(1, x)$$

.....

$$\frac{d}{dx}P(n, x) = -n\alpha P(n, x) + (n-1)\alpha P(n-1, x)$$

with the boundary conditions that we had a single electron at the beginning,

$$P(1, 0) = 1; P(n, 0) = 0, n > 1.$$

By successive integration we get

$$P(1, x) = e^{-\alpha x}$$

$$P(2, x) = e^{-\alpha x} (1 - e^{-\alpha x})$$

.....

$$P(n, x) = e^{-\alpha x} (1 - e^{-\alpha x})^{n-1}.$$

Taking into account that $e^{-\alpha x}$ is the mean value of n , \bar{n} , we get

$$P(n, x) = \frac{1}{\bar{n}} \left(1 - \frac{1}{\bar{n}}\right)^{n-1}.$$

which is for $n \gg 1$

$$P(n, x) = \frac{1}{\bar{n}} e^{-\frac{n}{\bar{n}}}.$$